National Library of Canada
Bibliothèque nationale du Canada

Canadian Theses Service
Services des thèses canadiennes

Ottawa, Canada
K1A 0N4

CANADIAN THESES
THÈSES CANADIENNES

NOTICE

The quality of this microfiche is heavily dependent upon the quality of the original thesis submitted for microfilming. Every effort has been made to ensure the highest quality of reproduction possible.

If pages are missing, contact the university which granted the degree.

Some pages may have indistinct print especially if the original pages were typed with a poor typewriter ribbon or if the university sent us an inferior photocopy.

Previously copyrighted materials (journal articles, published tests, etc.) are not filmed.

Reproduction in full or in part of this film is governed by the Canadian Copyright Act, R.S.C. 1970, c. C-30. Please read the authorization forms which accompany this thesis.

AVIS

La qualité de cette microfiche dépend grandement de la qualité de la thèse soumise au microfilmage. Nous avons tout fait pour assurer une qualité supérieure de reproduction.

S'il manque des pages, veuillez communiquer avec l'université qui a conféré le grade.

La qualité d'impression de certaines pages peut laisser à désirer, surtout si les pages originales ont été dactylographiées à l'aide d'un ruban usé ou si l'université nous a fait parvenir une photocopie de qualité inférieure.

Les documents qui font déjà l'objet d'un droit d'auteur (articles de revue, examens publiés, etc.) ne sont pas microfilmés.

La reproduction, même partielle, de ce microfilm est soumise à la Loi canadienne sur le droit d'auteur, SRC 1970, c. C-30. Veuillez prendre connaissance des formules d'autorisation qui accompagnent cette thèse.

THIS DISSERTATION
HAS BEEN MICROFILMED
EXACTLY AS RECEIVED

LA THÈSE A ÉTÉ
MICROFILMÉE TELLE QUE
NOUS L'AVONS REÇUE

Canada

NL 339 (r. 86/01)

158

National Library of Canada | Bibliothèque nationale du Canada

Canadian Theses Division | Division des thèses canadiennes

Ottawa, Canada
K1A 0N4

0-315-26890-5

PERMISSION TO MICROFILM — AUTORISATION DE MICROFILMER

• Please print or type — Écrire en lettres moulées ou dactylographier

Full Name of Author — Nom complet de l'auteur

Bruce Edmunds Roberts

Date of Birth — Date de naissance	Country of Birth — Lieu de naissance
Sept 25, 1953	CANADA

Permanent Address — Résidence fixe

418 · 12 Street S.E.
Medicine Hat, Alta.

Title of Thesis — Titre de la thèse

Solubility of Carbon Dioxide and Hydrogen Sulphide in Mixed and Chemical Solvents

University — Université

University of Alberta

Degree for which thesis was presented — Grade pour lequel cette thèse fut présentée

MSc

Year this degree conferred — Année d'obtention de ce grade	Name of Supervisor — Nom du directeur de thèse
1983	Dr. A.E. Mather

Permission is hereby granted to the NATIONAL LIBRARY OF CANADA to microfilm this thesis and to lend or sell copies of the film.

The author reserves other publication rights, and neither the thesis nor extensive extracts from it may be printed or otherwise reproduced without the author's written permission.

L'autorisation est, par la présente, accordée à la BIBLIOTHÈQUE NATIONALE DU CANADA de microfilmer cette thèse et de prêter ou de vendre des exemplaires du film.

L'auteur se réserve les autres droits de publication; ni la thèse ni de longs extraits de celle-ci ne doivent être imprimés ou autrement reproduits sans l'autorisation écrite de l'auteur.

Date	Signature
Oct 14/83	Bruce Roberts

NL-91 (4/77)

THE UNIVERSITY OF ALBERTA

Solubility of Carbon Dioxide and Hydrogen Sulphide in Mixed and Chemical Solvents

by

Bruce E. Roberts

(C)

A THESIS

SUBMITTED TO THE FACULTY OF GRADUATE STUDIES AND RESEARCH

IN PARTIAL FULFILMENT OF THE REQUIREMENTS FOR THE DEGREE

OF Master of Science

Chemical Engineering

EDMONTON, ALBERTA

Fall 1983

THE UNIVERSITY OF ALBERTA

RELEASE FORM

NAME OF AUTHOR Bruce E. Roberts

TITLE OF THESIS Solubility of Carbon Dioxide and Hydrogen Sulphide in Mixed and Chemical Solvents

DEGREE FOR WHICH THESIS WAS PRESENTED Master of Science

YEAR THIS DEGREE GRANTED Fall 1983

Permission is hereby granted to THE UNIVERSITY OF ALBERTA LIBRARY to reproduce single copies of this thesis and to lend or sell such copies for private, scholarly or scientific research purposes only.

The author reserves other publication rights, and neither the thesis nor extensive extracts from it may be printed or otherwise reproduced without the author's written permission.

(SIGNED) Bruce Roberts

PERMANENT ADDRESS:

418 12 Street S.E.

Medicine Hat, Alberta

Canada

DATED Oct. 14 1983

THE UNIVERSITY OF ALBERTA

FACULTY OF GRADUATE STUDIES AND RESEARCH

The undersigned certify that they have read, and recommend to the Faculty of Graduate Studies and Research, for acceptance, a thesis entitled Solubility of Carbon Dioxide and Hydrogen Sulphide in Mixed and Chemical Solvents submitted by Bruce E. Roberts in partial fulfilment of the requirements for the degree of Master of Science.

A.E. Mather
.....
Supervisor

.....

.....

Date October 7, 1983

Abstract

The solubility of hydrogen sulphide and carbon dioxide has been measured at 40 and 100°C in a mixed solvent of 16.5 wt% (2.0 M) 2-amino-2-methyl-1-propanol (AMP), 32.2% tetrahydrothiophene 1,1 dioxide (sulfolane), and 51.3% water. The solubility of hydrogen sulphide and carbon dioxide was also measured in a chemical solvent of 2.0 M aqueous AMP and in pure sulfolane to permit an assessment of the influence of the physical solvent component on the solubility of acid gases in mixed amine solvent systems.

At solution loadings less than 1 mol acid gas/mol AMP, the solubility of the acid gas was lower in the mixed solvent than in the corresponding aqueous AMP solvent. At solution loadings greater than 1 mol acid gas/mol AMP, the solubility of the gases in the mixed solvent surpassed the solubility in the corresponding aqueous system. The experimental results are rationalized in terms of the solvent effects on the chemical reaction and physical vapour-liquid equilibria. The solubility model of Deshmukh and Mather was modified to account for the solvent effects on the equilibria. The model predictions were in satisfactory agreement with the experimental results.

Acknowledgments

I wish to thank my supervisor, Dr. A.E. Mather, who broadened my interest in thermodynamics and provided support over the course of my graduate program. Dr. F.Y. Jou assisted in the design of the experimental procedure. K. Faulder, R. Scott, J. Van Doorn, R. Van den Heuvel, D. Sutherland, J. McDonald, and A. Koenig were involved in the assembly of the experimental apparatus. I am grateful to Dr. F.D. Otto and Dr. L.G. Hepler who reviewed the thesis and suggested improvements. Financial support from the University of Alberta, the National Research Council, and the Alberta Research Council is gratefully acknowledged. Finally, I wish to express my gratitude to my friend, Tamsen Wolcott, for encouraging me to return to university and for support through the duration of the program.

Table of Contents

Chapter		Page
1.	INTRODUCTION	1
2.	GENERAL BACKGROUND	7
	2.1 Thermodynamics and Chemistry of Acid Gas Absorption	7
	2.2 Literature Survey	10
3.	EXPERIMENTAL PROCEDURES	14
	3.1 Survey of Experimental Methods	14
	3.2 Description of Experimental Apparatus	17
	3.3 Experimental Procedure	20
	3.3.1 Establishment of equilibrium	20
	3.3.2 Vapour phase analysis	22
	3.3.3 Liquid phase analysis	23
	3.3.4 Materials	26
4.	EXPERIMENTAL RESULTS AND DISCUSSION	28
	4.1 Preliminary Results	28
	4.2 Experimental Results	31
	4.3 Accuracy of Data	40
	4.4 Discussion of Experimental Results	41
5.	CORRELATION OF EXPERIMENTAL DATA	44
	5.1 Survey of Models	44
	5.2 Correlation of Acid Gas Solubility in Aqueous AMP	48
	5.3 Correlation of Solubility in Mixed AMP	52
	5.4 Predictive Application of Solubility Model	54
	5.5 Discussion of Correlative Model	58
6.	CONCLUSIONS	65

References 67

Appendix 1. Gas Chromatograph Calibration 71

Appendix 2 - Calculation of Solubility from Measured Quantities 73

Appendix 3 - Raw Experimental Data 76

Appendix 4 - Error Analysis 84

Appendix 5 - Thermodynamic Framework 88

Appendix 6 - Solubility Model Predictions 91

List of Tables

Table		Page
1.	Solubility of CO_2 in 3.0 M Aqueous AMP at 40°C	28
2.	Solid Formation in Mixed Solvent at 40°C and 5500 kPa	30
3.	Solubility of CO_2 at 40 and 100°C in 2.0 M Aqueous AMP	32
4.	Solubility of CO_2 at 40 and 100°C in 2.0 M Mixed Solvent	32
5.	Solubility of H_2S at 40 and 100°C in 2.0 M Aqueous AMP	33
6.	Solubility of H_2S at 40 and 100°C in 2.0 M Mixed Solvent	33
7.	Solubility of CO_2 at 40 and 100°C in Sulfolane	34
8.	Solubility of H_2S at 40 and 100°C in Sulfolane	34
9.	Henry's Constants for CO_2 and H_2S in Sulfolane	37
10.	Henry's Constants and Equilibrium Constants in Mixed Solvent at 40 and 100°C	55
11.	Equilibrium Constants for Overall Reactions in Mixed and Aqueous AMP	61
A1.1	Variation of CO_2 Response Factors with Composition	72
A1.2	Variation of H_2S Response Factors with Composition	72
A3.1	Raw Data - Solubility of CO_2 in 3.0 M Aqueous AMP at 40°C	77
A3.2	Raw Data - Solubility of CO_2 in 2.0 M Mixed Solvent at 100°C	78
A3.3	Raw Data - Solubility of CO_2 in 2.0 M Mixed Solvent at 40°C	78

Table		Page
A3.4	Raw Data - Solubility of CO_2 in 2.0 M Aqueous AMP at 40°C	79
A3.5	Raw Data - Solubility of CO_2 in 2.0 M Aqueous AMP at 100°C	79
A3.6	Raw Data - Solubility of H_2S in 2.0 M Mixed Solvent at 40°C	80
A3.7	Raw Data - Solubility of H_2S in 2.0 M Mixed Solvent at 100°C	80
A3.8	Raw Data - Solubility of H_2S in 2.0 M Aqueous AMP at 100°C	81
A3.9	Raw Data - Solubility of H_2S in 2.0 M Aqueous AMP at 40°C	81
A3.10	Raw Data - Solubility of CO_2 in Sulfolane at 40°C	82
A3.11	Raw Data - Solubility of CO_2 in Sulfolane at 100°C	82
A3.12	Raw Data - Solubility of H_2S in Sulfolane at 40°C	83
A3.13	Raw Data - Solubility of H_2S in Sulfolane at 100°C	83
A6.1	Predicted Partial Pressure of CO_2 in Aqueous and Mixed AMP Solutions at 40 and 100°C	92
A6.2	Predicted Partial Pressure of H_2S in Aqueous and Mixed AMP Solutions at 40 and 100°C	93
A6.3	Predicted Solubility of H_2S in 2.0 M Mixed Solvent at 40°C as a Function of H_2S and CO_2 Loading	94
A6.4	Predicted Effect of Temperature on the Solubility of H_2S in 2.0 M Mixed Solvent	95
A6.5	Molality of Liquid Phase Species in 2.24 molal Mixed Solvent at 40°C as a Function of H_2S Loading	96
A6.6	Molality of Liquid Phase Species in 2.24 molal Aqueous AMP at 40°C as a Function of H_2S Loading	97

Table		Page
A6.7	Molality of Liquid Phase Species in 2.24 molal Mixed Solvent at 100°C as a Function of H_2S Loading	98
A6.8	Molality of Liquid Phase Species in 2.24 molal Aqueous AMP at 100°C as a Function of H_2S Loading	99
A6.9	Molality of Liquid Phase Species in 2.24 molal Mixed AMP at 40°C as a Function of CO_2 Loading	100
A6.10	Molality of Liquid Phase Species in 2.24 molal Aqueous AMP at 40°C as a Function of CO_2 Loading	101
A6.11	Molality of Liquid Phase Species in 2.24 molal Mixed AMP at 100°C as a Function of CO_2 Loading	102
A6.12	Molality of Liquid Phase Species in 2.24 molal Aqueous AMP at 100°C as a Function of CO_2 Loading	103

List of Figures

Figure		Page
1.	Basic flowsheet for acid gas removal	2
2.	Experimental apparatus	18
3.	Solubility of CO_2 in 3.0 M aqueous AMP at 40°C	29
4.	Solubility of CO_2 in mixed and aqueous AMP	35
5.	Solubility of H_2S in mixed and aqueous AMP	36
6.	Solubility of CO_2 in sulfolane	38
7.	Solubility of H_2S in sulfolane	39
8.	Physical solubility of H_2S in mixed and aqueous AMP	42
9.	Comparison of predicted and experimental H_2S solubility in aqueous AMP	50
10.	Comparison of predicted and experimental CO_2 solubility in aqueous AMP	51
11.	Comparison of predicted and experimental H_2S solubility in mixed AMP	56
12.	Comparison of predicted and experimental CO_2 solubility in mixed AMP	57
13.	Predicted effect of temperature on solubility of H_2S in mixed AMP	59
14.	Predicted effect of CO_2 loading on solubility of H_2S in mixed AMP solution at 40°C	60
15.	Concentration of liquid phase species at 40°C as a function of H_2S loading	63
16.	Concentration of liquid phase species at 100°C as a function of H_2S loading	64

Nomenclature

a	activity
b	constant in Debye-Hückel expression
f	fugacity, Pa
m	molality, mol/kg
$\bar{v}$	partial molar volume, m^3/mol
x	mole fraction in liquid phase
y	mole fraction in vapour phase
z	electric charge
A	constant in Debye-Hückel expression
A	Margules constant
H	Henry's constant
H	enthalpy, J/mol
I	ionic strength, mol/kg
I	integration constant
K	chemical equilibrium constant
P	pressure, Pa
R	gas constant, J/mol K
T	temperature, K

Greek letters

α	mole ratio in liquid
β	binary interaction parameter
γ	activity coefficient
ϕ	fugacity coefficient

Subscripts

i	component i
j	component j
m	mixture
w	water
A	component A
1	acid gas component
2	physical solvent component
3	chemical solvent component

Superscripts

l	liquid
s	saturated conditions
v	vapour
°	reference state

1. INTRODUCTION

Acid gas impurities such as CO_2 and H_2S occur in significant quantities in the gas streams of many industrial processes. Natural gas purification, coal gasification, ammonia manufacture, and hydrogen production are examples of such processes. The nature of the process and the acid gas determine the degree to which the impurity must be removed. Due to the toxicity and corrosiveness of H_2S and its ability to poison catalysts, the removal requirement for H_2S is often severe. For a number of situations, CO_2 must also be removed to prevent catalyst poisoning and to reduce the quantity of CO_2 acting as a diluent in the treated gas.

A widely used method for acid gas removal is the absorption of the acidic components into a liquid. The flowsheet shown in Figure 1 outlines the basis of acid gas removal by this process. The raw gas containing the impurity enters the bottom of the absorption tower and is contacted countercurrently with the solvent. The treated gas exits from the top of the tower for further processing. The liquid containing the acid gas (rich solvent) is flashed to desorb the hydrocarbons, heated, and fed to the top of the regeneration column. A reboiler heated with low pressure steam generates vapour which contacts the liquid proceeding down the column. The water-saturated acid gases which have been stripped from solution are cooled to condense most of the water which is returned to the column. The acid gas is sent on for further treatment such as elemental sulphur

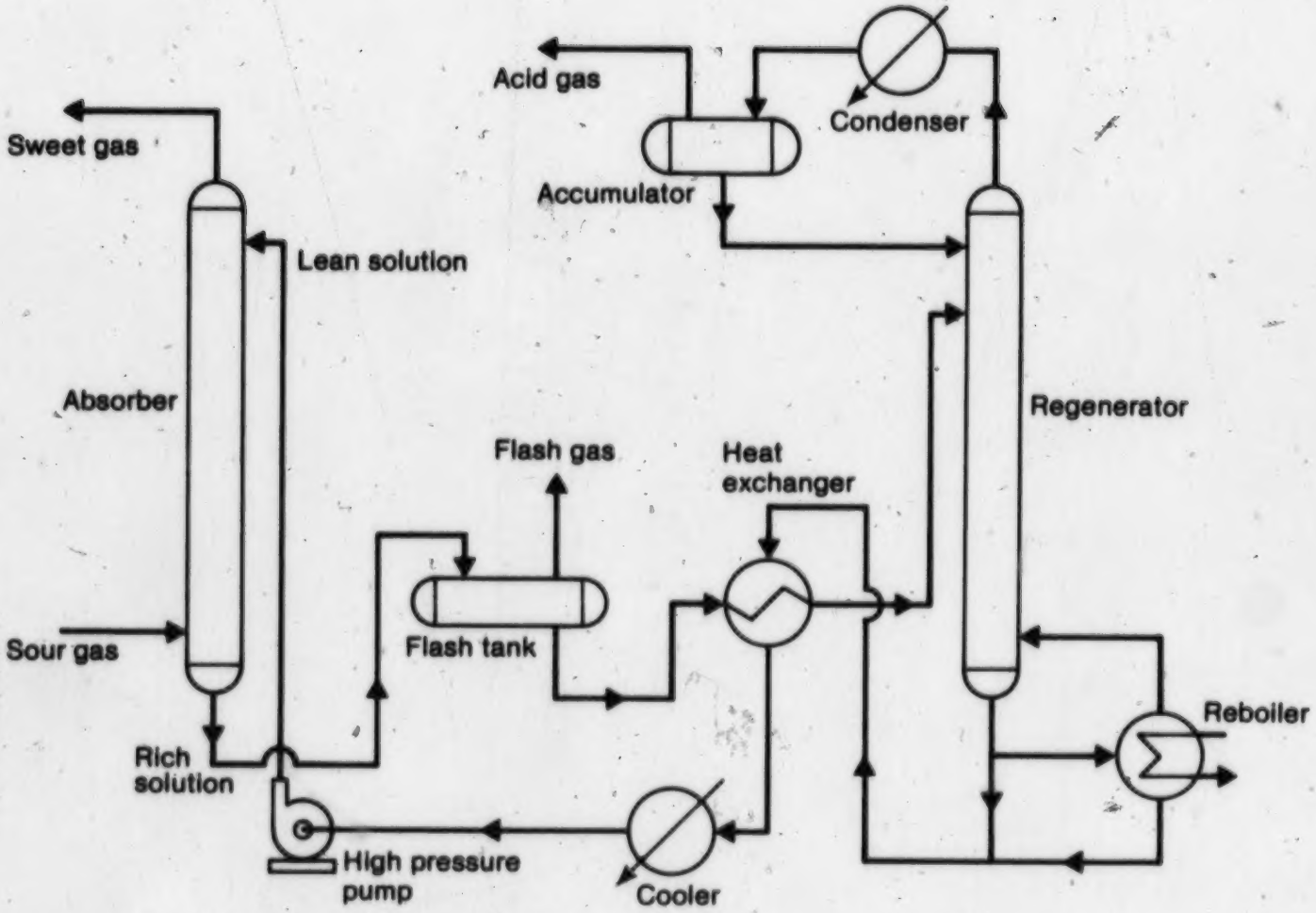

Figure 1. Basic flowsheet for acid gas removal.

recovery. The solvent which has been stripped of the soluble gas (lean solvent) is cooled and fed to the top of the absorption unit.

The solvent should have several important properties to be considered for use in the absorption process. The solvent must have a high capacity for the acid gas under absorption conditions but have a significantly lower capacity under regeneration conditions. The difference in solubility between the two stages establishes the circulation rate of the solvent which in turn influences the equipment sizes and heat requirements for regeneration. Reduced heat duties are also favored by a low heat of desorption and low solvent heat capacity. Furthermore, the solvent must have a low vapour pressure to reduce solvent losses and a low capacity for hydrocarbons which, if absorbed with the acid gas, may lead to catalyst fouling in the sulphur recovery unit.

The solvents for acid gas removal may be categorized in terms of the mechanism of absorption. The most widely used are chemical solvents which are characterized by liquid phase reactions between the acid gas and a soluble base. Examples of chemical solvents are aqueous solutions of monoethanolamine (MEA), diethanolamine (DEA), and diglycolamine (DGA). The chemical reaction allows for a high solubility even at low partial pressures. The solubility, however, is limited by the stoichiometry of the reaction, and the solution can not be easily loaded once the reactant has been depleted.

A second major group of absorbents are the physical solvents in which absorption occurs strictly by physical dissolution. Examples of physical solvents for acid gas removal are methanol, N-methyl pyrrolidone, and propylene carbonate. The solubility is approximately linear with partial pressure. Thus, these solvents have a much lower capacity for the acid gases than chemical solvents at low partial pressures, but as they lack the stoichiometric limits, may be loaded to higher levels at high partial pressures. Regeneration of the solvent may be accomplished by pressure reduction thereby reducing the energy requirements of the process. An important disadvantage of physical solvents arises from their higher capacity for hydrocarbons.

A much smaller class of absorbents are the mixed solvents which are comprised of a chemically reactive component and a physical solvent with a high capacity for the acid gases. [1] The development of mixed solvents arises from an attempt to combine the desirable features of physical and chemical solvents. The replacement of a portion of the water of the aqueous chemical solvent with a physical solvent should have two effects. The solubility should not be severely limited by stoichiometry and a higher solubility at high partial pressures should be realized. Secondly, the solvent should be more readily regenerated owing to the

---

[1] Aqueous chemical solvents may be classified as mixed solvents. In this study, however, the term is reserved for mixtures containing a physical solvent that has a much higher capacity for the acid gases than water.

reduced heat of desorption and heat capacity.

Operating details have been outlined on several industrially used mixed solvents. A widely used mixed solvent, Sulfinol, is composed of diisopropanolamine (chemical component), sulfolane (physical solvent), and water. (Dunn et al., 1964). The Amisol process (Bratzler and Doerges, 1974) uses a mixed solvent of MEA or DEA (chemical component), methanol (physical solvent), water, and an unspecified additive. Solubility data for these solvents have not been released.

The solubility of CO_2 and H_2S in physical and chemical solvents has been investigated over a wide range of temperatures and partial pressures. Few experimental studies, however, have been reported on the solubility of CO_2 and H_2S in mixed solvents. Such data are required to assess the feasibility of applying mixed solvents in processes currently using chemical or physical solvents. The objective of this study was to provide solubility data on a mixed solvent system at typical absorption and regeneration temperatures and over a wide range of partial pressures. The mixed solvent studied was composed of an amine, 2-amino-2-methyl-1-propanol (AMP), a physical solvent, tetrahydrothiophene 1,1 dioxide (sulfolane), and water. Aqueous AMP has been recently reported to have important advantages over the more traditional amines. The solubility in an aqueous solution of AMP and in pure sulfolane was also measured to permit an evaluation of the influence of the

physical solvent component in the mixed system.

Background information on the solubility of acid gases in chemical, physical, and mixed solvents is outlined in Chapter 2. Chapter 3 presents a description of the experimental procedures used to obtain the data. Experimental results are presented and discussed in Chapter 4. A model used to correlate the solubility data and to predict solubility under different conditions is described and discussed in Chapter 5. Finally, the conclusions which may be drawn from the results of the solubility experiments and correlative model are summarized in Chapter 6.

2. GENERAL BACKGROUND

2.1 Thermodynamics and Chemistry of Acid Gas Absorption

Equilibria involving physical and chemical solvents may be represented as:

$A(g)$	$A(g)$
$\|\|$	$\|\|$
$A(l)$	$A(l) + B = \text{ions}$
physical solvent	chemical solvent

For the physical solvent, only the vapour-liquid equilibrium for the molecular species A need be considered. At equilibrium, the fugacity of A in the vapour and liquid phases are equal:

$$f_A^v = f_A^l \tag{2.1}$$

The fugacity of a component in the vapour is most commonly expressed in the form of Equation (2.2):

$$f_A^v = \phi_A y_A P \tag{2.2}$$

The liquid phase fugacity may be written as:

$$f_A^l = \gamma_A m_A H_A e^{\int_{P^s}^{P} \frac{\bar{V}_A}{RT} dP} \tag{2.3}$$

The Henry's constant, H, is defined as:

$$H_A = \lim_{m_A \to 0} \frac{f_A}{m_A}$$

The exponential term in Equation (2.3), the Poynting correction factor, accounts for the effect of pressure on the liquid phase fugacity and may be neglected except at high pressures.

Substituting Equations (2.2) and (2.3) for the fugacity in Equation (2.1) yields:

$$\phi_A y_A P = \gamma_A m_A H_A e^{\int_{P^S}^{P} \frac{\bar{v}_A}{RT} dP} \qquad (2.4)$$

If the assumptions of ideal gas and ideal solution are made, Equation (2.4) simplifies to:

$$y_A P = m_A H_A \qquad (2.5)$$

Thus the partial pressure of A will vary approximately linearly with liquid molality.

The thermodynamics of the chemical solvent system is more complex. As in the physical solvent, physical equilibrium exists between the phases for the molecular component. Chemical equilibrium must also be considered for each liquid phase reaction. The overall reaction between an amine and H_2S may be written as:

$$H_2S + RNH_2 = HS^- + RNH_3^+ \quad (2.6)$$

Two overall reactions for CO_2 may be written:

$$RNH_2 + CO_2 + H_2O = RNH_3^+ + HCO_3^- \quad (2.7)$$

$$CO_2 + 2RNH_2 = RNHCOO^- + RNH_3^+ \quad (2.8)$$

Tertiary amines do not form carbamates ($RNHCOO^-$) and react with CO_2 by Equation (2.7) alone.

The chemical equilibrium for the general reaction:

$$aA + bB = cC + dD \quad (2.9)$$

may be expressed as :

$$K = \frac{m_C^c \; m_D^d}{m_A^a \; m_B^b} \cdot \frac{\gamma_C^c \; \gamma_D^d}{\gamma_A^a \; \gamma_B^b} \quad (2.10)$$

The equilibrium favors the formation of the ionic species. In solutions of excess amine, only a small portion of the acid gas absorbed is present as the molecular species, and thus the partial pressure above the solution is low. At a loading of 1 mol/mol amine, the concentration of undissociated amine is low and the partial pressure rises rapidly as the molality of the molecular species increases. Beyond this stoichiometric point, only a small fraction of

the acid gas absorbed reacts, and the system behaves like the physical solvent.

Consideration of the two reactions for CO_2 absorption indicates that the formation of a stable carbamate would limit the maximum loading to 0.5 mol/mol amine. Primary and secondary amines such as MEA and DEA do exhibit a reluctance to load up beyond this point, although high loadings are observed at high pressures. A stoichiometric limit of 1 mol/mol amine is possible for tertiary amines such as MDEA which do not form carbamates. The absorption rates, however, for these amines are low, thus limiting their industrial importance. Sartori and Savage (1982) have recently reported on the use of a sterically hindered primary amine, 2-amino-2-methyl-1-propanol (AMP) for absorption of CO_2. By placing a bulky group next to the nitrogen, the carbamate is destabilized and the maximum stoichiometric loading may be realized.

2.2 Literature Survey

In contrast to the large number of studies on the solubility of acid gases in aqueous amine solutions, few experimental studies have been reported for mixed solvent systems. Furthermore, the studies which have investigated mixed solvents have often been restricted to a narrow pressure and temperature range.

Several authors have reported on the solubility of acid gases in nonaqueous mixtures of amines and organic solvents.

Leites et al. (1972) measured the solubility of CO_2 at 20°C and partial pressures less than 100 kPa in solutions of MEA (2.5 M) and various organic solvents. All mixed solvents examined exhibited a lower capacity for CO_2 than the corresponding 2.5 M aqueous solution of MEA. Of the systems examined, the MEA-methanol mixture yielded the highest capacity for CO_2. This reduced capacity of the nonaqueous mixed solvent at low partial pressures was later confirmed by Rivas (1978) who measured acid gas solubility in nonaqueous mixtures of sulfolane, propylene carbonate, and N-methyl pyrrolidone with MEA and DGA.

At higher partial pressures, the solubility in the nonaqueous mixed solvent has been observed to be greater than the corresponding aqueous system. Banasiak (1981) measured the solubility of CO_2 in 15 wt % MEA and 85% methanol at 30°C and partial pressures from 225 kPa to 325 kPa. Under these conditions, the solubility in the mixed solvent is approximately 25% higher than in an aqueous solution of 15% MEA.

Several investigations on three component solutions consisting of an amine, a physical solvent, and water have also been reported. Woertz (1972) presented results for a series of mixtures at 27°C and partial pressures from 425 to 670 kPa. The amines examined, MEA, DEA, and DIPA, were held at a constant concentration of 1.5 M. The solubility of CO_2 in blends of MEA, water (3-10% by volume), and either dimethyl formamide, methyl pyrrolidone, or diethylene glycol

was greater than in the corresponding aqueous solutions. Mixtures with other physical solvents such as sulfolane, dimethyl ethers of diethylene and triethylene glycol, and methyl carbitol exhibited a lower capacity for CO_2. This reduced solubility in the mixed solvent was even more apparent for DIPA. No explanation for this decreased solubility was proposed.

The solubility of CO_2 in mixtures of MEA, sulfolane, and water at 30°C and partial pressures less than 100 kPa was measured by Yushko et al. (1973). The MEA concentration was maintained at 2.5 M while the sulfolane content varied from 0 to 84 wt %. The solubility of CO_2 decreased as the sulfolane content of the solvent increased. This trend at low pressures was also observed by Dimov et al. (1976) for mixtures of MEA, water, and ethylene glycol or N-methyl pyrrolidone.

The solubility of CO_2 and H_2S at 40 and 100°C in a Sulfinol solution (40 wt. % DIPA, 40% sulfolane, and 20% water) was measured by Isaacs et al. (1977) at partial pressures from 2.4 to 5700 kPa. Solubility data for an aqueous solution of DIPA with the same concentration were not reported, and therefore, the influence of the solvent could not be accurately assessed.

Several generalizations on the solubility of acid gases in mixed solvents may be drawn from this survey. At low partial pressures (less than 100 kPa), the replacement of some or all of the water by a physical solvent appears to

reduce the solubility of the acid gases. This reduction increases as the water content decreases. At higher pressures, certain physical solvents, such as methanol, enhance the capacity for CO_2 or H_2S. Data on the solubility in mixed and corresponding aqueous solvents over a wide range of pressures are lacking.

3. EXPERIMENTAL PROCEDURES

3.1 Survey of Experimental Methods

The solubility of CO_2 and H_2S in amine solutions has been determined experimentally by numerous methods. These methods generally involve contacting the acid gas with the liquid at constant temperature until equilibrium has been reached, at which point the vapour and liquid phases are analyzed. The experimental methods differ in the manner in which the phases are contacted and in the analytical method employed. The choice of experimental method is often determined by the range of acid gas partial pressure for which the solubility data are desired.

The solubility in aqueous amine solutions for a wide range of acid gas partial pressure may be determined by bringing the vapour and liquid phases to equilibrium in a static equilibrium cell. The cells are fitted with liquid and vapour sample lines, and the cell pressure is continuously monitored. Equilibrium is indicated when a constant cell pressure is observed.

A rocking autoclave cell contained in a liquid constant temperature bath was used by Jones et al. (1959) and Lawson and Garst (1976) in their determination of the solubility of acid gases in MEA and DEA. Reed and Wood (1941) used a stirred autoclave to saturate MEA and DEA solutions with CO_2. The large internal volume of these cells allows for large fluid samples to be taken and hence permits

determination of the solubility at very low partial pressures. An equilibrium cell comprised of a stainless steel cylinder fitted with a magnetic stirrer was used by Lee et al. (1972).

A disadvantage of the these cells arises from the inability to visually observe the fluid phases and to detect liquid phase immiscibility. An improvement in the design of the apparatus was outlined by Lee et al. (1973) who used a visual equilibrium cell consisting of a Jerguson gauge connected to a 250 cm^3 vapour reservoir. A magnetic pump was used to recirculate the vapour from the gas reservoir back through the liquid in the cell. This apparatus was judged to be most suitable for the purposes of this study. Other experimental equipment reported in the literature, such as the gas flow apparatus described by Nasir and Mather (1977), are unsuitable for this study as they are limited to pressures lower than 100 kPa.

The selection of the analytical method may now be considered. Lawson and Garst and Jones et al. analyzed the vapour phase, which had been sampled into an evacuated bomb, by mass spectrometry. Lee et al. (1972) sampled the vapour phase directly into the sample loop of a gas chromatograph. This method of analysis was adopted in this study. In both methods, the results are reported in mole percent on a water-free basis; thus an estimate of the water partial pressure over the amine/water solution is required.

Several analytical methods for the determination of the acid gas concentration in the liquid phase have been outlined. The most common method of analysis for CO_2 is to acidify the liquid sample and measure the amount of CO_2 which is evolved. Reed and Wood and Lee et al. (1972) measured the amount evolved by accurately determining the vapour volume and from PVT data, calculating the equivalent mass of CO_2. Mason and Dodge (1936), Jones et al., and Lawson and Garst adsorbed the CO_2 onto a selective adsorbent. The mass of CO_2 evolved was determined by reweighing the adsorbent material.

A more direct method of analysis for CO_2, described by Jou et al. (1982), was selected for this study. The liquid sample was withdrawn from the cell and injected into an excess of sodium hydroxide solution. The amount of carbonate in the sample was determined by adding a solution of $BaCl_2$ and precipitating the carbonate as $BaCO_3$:

$$Ba^{+2} + CO_3^{-2} = BaCO_3 \qquad (3.1)$$

The precipitate was analyzed by titrating with standard acid:

$$BaCO_3 + 2H^+ = CO_2 + Ba^{+2} + H_2O \qquad (3.2)$$

Hydrogen sulphide has been most commonly analyzed by iodimetric techniques. An aliquot sample is added to an

acidified solution of excess iodine. The reaction may be represented as:

$$I_3^- + H_2S = S + 3I^- + 2H^+ \qquad (3.3)$$

The unreacted iodine is determined by titrating with thiosulphate:

$$2S_2O_3^{-2} + I_3^- = S_4O_6^{-2} + 3I^- \qquad (3.4)$$

By knowing the amount of iodine which reacts, the amount of sulphide in the sample may be calculated.

3.2 Description of Experimental Apparatus

The equipment permitted solubility measurements to be taken at acid gas partial pressures from 1 to 7000 kPa and temperatures from 25 to 130°C. A schematic diagram of the apparatus is shown in Figure 2. The liquid and vapour phases were brought to equilibrium in a windowed Jerguson cell. The cell had an internal volume of approximately 75 cm^3 and a maximum pressure rating of 7000 kPa at 40°C. Pyrex windows were sealed to the metal surface by asbestos gaskets. A 250 cm^3 cylindrical reservoir was attached to the top of the cell to increase the mass of vapour in equilibrium with the solvent.

The vapour from the reservoir was recirculated through the solvent by a magnetically driven pump devised by Ruska

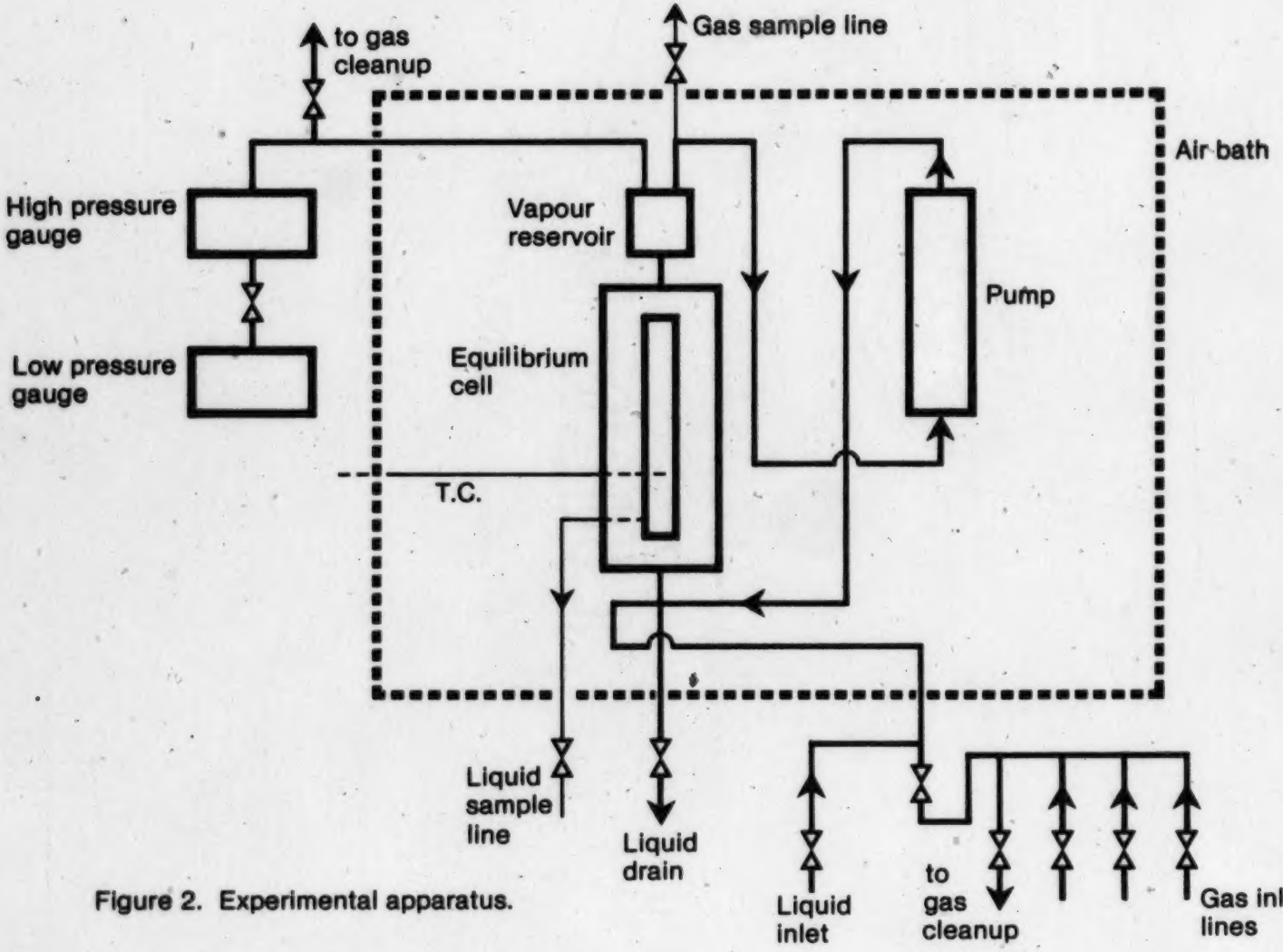

Figure 2. Experimental apparatus.

et al. (1970). A free piston, fitted with a check valve and fluid passages, moved up and down within the cylinder through the action of a magnetic sleeve. The sleeve was driven by a 0.25 hp Boston Gear motor through a connecting rod. The pump discharged on the upstroke of the piston transporting the vapour from the reservoir to the bottom of the equilibrium cell. The pump was connected to the reservoir and equilibrium cell by 1/8 in (3.18 mm) OD type 316 stainless steel tubing.

With the exception of the pump piston, all materials in contact with the fluid were manufactured from type 316 stainless steel. The piston was made from Carpenter 450 steel as it must be ferromagnetic. The cell and pump were housed in a 0.4 m^3 air bath maintained at ±0.1°C of the setpoint temperature by a Thermo Electric temperature controller. The heater was comprised of a series of electrically heated fins which allowed for measurements to be obtained to 130°C. The air bath was also provided with a copper cooling coil through which cold water circulated thus permitting solubility measurements to 25°C. The air within the bath was mixed by a blade fan.

The temperature of the fluid within the cell was monitored by a calibrated iron-constantan thermocouple which extended through the cell into the fluid. The thermocouple was calibrated against a Leeds and Northrup platinum resistance thermometer in the temperature range of interest. A Leeds and Northrup potentiometer was used to measure the

thermocouple output.

High cell fluid pressure was measured by a 0 to 10 000 kPa digital Heise gauge. At low pressures, a 0 to 1 000 kPa digital Heise gauge was used. The accuracy of both gauges was rated at ±0.1% of the full scale span and was checked with a Ruska 2400 HL dead weight tester. The gauges were connected to the Jerguson cell by 1/8 in (3.18 mm) OD stainless steel tubing.

The gas and liquid sample lines were stainless steel tubes of 1/16 in (1.59 mm) OD. The gas sample line extended from the reservoir to a valve external to the air bath. A tube extended from the outlet of the valve to the sample loop of the gas chromatograph. The liquid sample line led from a port 5 cm from the base of the cell to a needle valve located outside of the air bath.

Due to its extreme toxicity, H_2S must not be vented directly to the atmosphere. An absorption train comprised of two 2 litre glass vessels containing 6 M sodium hydroxide removed the H_2S from the gas which had been released from the apparatus. The effluent from the absorption train was vented to a fume hood.

3.3 Experimental Procedure

3.3.1 Establishment of equilibrium

The apparatus was brought to the desired temperature and purged for 1 hour to remove traces of oxygen.

Approximately 50 cm^3 of the solvent was fed by gravity to the equilibrium cell. CO_2 or H_2S was added to the cell through the gas inlet valve to an amount monitored by the pressure gauge. The valve was closed and the pump started. As the vapour recirculated through the solvent, the acid gas was absorbed into the solvent and the system pressure decreased as equilibrium was approached. Additional amounts of acid gas were added until the desired partial pressure had been approximately obtained. If necessary, nitrogen was added to maintain the system pressure above 350 kPa.

The vapour was recirculated until the pressure remained constant for several hours thus indicating the establishment of equilibrium. The period of time necessary to reach equilibrium decreased with an increase in temperature and solution loading. The equilibration time was also greater for absorption in the systems containing the amine than in pure sulfolane.

Equilibrium may be approached by adding acid gas to an undersaturated solution, as described above, or by desorbing the gas from a supersaturated solution by pressure reduction. Solubility measurements were obtained by both methods for all cases except the mixed and aqueous AMP solutions at 100°C. In these cases, gas was not released so as to prevent water loss from the solution.

When equilibrium had been reached, the pump was stopped and the cell pressure and temperature and barometric pressure recorded. The vapour and liquid phases were then

analyzed.

3.3.2 Vapour phase analysis

The analysis was carried out using a model 5710A Hewlett Packard gas chromatograph. The operating conditions were:

column temperature:	95 °C (CO_2 analysis)
	110 °C (H_2S analysis)
detector temperature:	150 °C
sample loop volume:	0.50 cm^3
column dimensions:	10 ft (3.0 m) X 1/4 in (6.35 mm) OD
column packing:	80-100 mesh Chromosorb 104
detector current:	100-140 mA
carrier gas flow:	30 cm^3/min He

The gas sample line and sample loop were initially flushed by releasing a small portion of the equilibrium vapour. The cell pressure generally dropped 5 to 10 kPa during this step. An eight port Valco gas sampling valve was then used to inject the sample loop contents into the chromatograph column. The relative amounts of the separated gases were measured using a thermal conductivity detector. The response from the detector was transmitted to a model 3380A Hewlett Packard integrator and the results reported in

terms of percent peak area.

Response factors were determined from the analysis of gas mixtures of CO_2 and H_2S with nitrogen. Details on the calculation of the response factors are outlined in Appendix 1. Using the values for the response factor and area percentage, the mole percentage of the acid gas on a water-free basis was determined.

The partial pressure of the water over the aqueous and mixed AMP solutions was calculated by assuming Raoult's law for the vapour-liquid equilibrium:

$$P_w = x_w P_w^s \qquad (3.5)$$

A sample calculation of the determination of the acid gas partial pressure from measured quantities is shown in Appendix 2.

3.3.3 Liquid phase analysis

The liquid sample was withdrawn from the equilibrium cell into a vessel containing a solution of 1 M sodium hydroxide, thus converting the free CO_2 and H_2S to the involatile ionic species. At high loadings of CO_2, the reaction rate was not great enough to prevent a pressure buildup above the caustic solution. Thus, a 40 cm^3 high pressure sample bomb containing the sodium hydroxide was used for the sampling of solutions containing CO_2 at partial pressures over 1000 kPa. The liquid sample valve was

connected to a tube which extended through the fitting in the stem to a point near the bottom of the cylinder. A 50 cm^3 Erlenmeyer flask fitted with a rubber septum served as a collection vessel for the sampling of CO_2 at partial pressures less than 1000 kPa and for the sampling of solutions containing H_2S.

The collection vessel was weighed to the nearest 0.1 mg on an analytical balance. Approximately 35 cm^3 of 1 M sodium hydroxide was added to the vessel and the vessel reweighed. About two cm^3 of the equilibrium liquid was withdrawn from the cell and flushed through the sample lines. The end of the sample line was then pushed through the rubber septum into the caustic solution in the flask, or for the cases noted previously, the line was attached to the high pressure sample bomb. As the collection vessel was agitated, the needle valve was opened slightly and the liquid sample allowed to flow into the caustic solution. The volume of the liquid sample taken depended upon the loading in the solution and ranged from 2 to 8 cm^3. The vessel was reweighed to obtain the mass of sample collected. The contents of the vessel were transferred quantitatively to a 100 cm^3 volumetric flask and diluted to the fiducial mark. Aliquot samples from 5 to 25 cm^3 were used for the determination of the carbonate or sulphide concentrations.

<u>H_2S analysis</u>

To a 250 cm^3 flask were added 5 to 10 cm^3 of 5 N H_2SO_4, 50 cm^3 of distilled water, and a pipetted volume of 0.100 N

iodine. Typically, 20 to 25 cm^3 of iodine were used. An aliquot sample of the basic sulphide solution was added with stirring to the iodine solution. The tip of the pipette was placed directly into the iodine solution to prevent the loss of H_2S. The volume of the aliquot sample was chosen such that the iodine would be present in excess. The solution was then titrated with standard 0.100 N sodium thiosulphate until the solution had turned pale yellow. Several drops of CS_2 and starch indicator were added. At this point, the CS_2 phase in the solution was pink and the bulk of the solution was blue due to the presence of unreacted iodine. The titration was continued with vigorous stirring until the blue and pink colors had disappeared.

A sample calculation of the determination of H_2S in the liquid is outlined in Appendix 2.

CO_2 analysis

An aliquot sample was pipetted into a 250 cm^3 Erlenmeyer flask. Approximately 50 cm^3 of 1 M $BaCl_2$ was added and the flask stoppered and allowed to stand for at least 12 hours. The barium carbonate precipitate was filtered using #6 Whatman paper and a 75 mm glass funnel. During the filtration, the funnel was covered with a glass watchglass to prevent CO_2 absorption from the atmosphere into the solution. The precipitate was washed with distilled water until the pH of the filtrate was approximately 5.9 as indicated by Duotest pH paper. Generally, this required 250 to 300 cm^3 of water. The precipitate and filter paper were

transferred to a 250 cm^3 Erlenmeyer flask containing 50 cm^3 of distilled water. The filter paper was shredded with a magnetic stirring bar. Five drops of methyl orange-xylene cyanol indicator were added and the suspension titrated with standard 0.100 N HCl to a grey green endpoint.

A sample calculation of the determination of CO_2 in a liquid sample is outlined in Appendix 2.

Amine analysis

A 20 cm^3 aliquot sample of the amine solution was pipetted into a 250 cm^3 Erlenmeyer flask. Several drops of methyl red indicator and 100 cm^3 of water were added. The solution was titrated with standard 1.00 N HCl to a light pink endpoint. The amine concentrations are reported at 23°C.

3.3.4 Materials

The aqueous amine solutions were prepared from distilled water and practical grade AMP (98% purity) supplied by Matheson, Coleman, and Bell. The sulfolane, supplied by Aldrich, had a purity of 99%. Both chemicals were used without purification.

The 1 M sodium hydroxide solution was prepared from reagent grade sodium hydroxide and degassed distilled water. The carbonate content was determined to be 2.0×10^{-4} moles carbonate per gram of solution. Certified standard solutions of hydrochloric acid, sodium thiosulphate, and iodine were used in the titrations. The barium solution was prepared from commercially purified barium chloride and distilled

water. The solution was filtered prior to use.

The N_2, CO_2, and H_2S gases were supplied by Matheson and had purities of 99.99%, 99.9%, and 99.5% respectively.

4. EXPERIMENTAL RESULTS AND DISCUSSION

4.1 Preliminary Results

The equilibrium solubility of CO_2 in 3.0 M aqueous AMP solution was measured at 40°C to provide a comparison with the values obtained by Sartori and Savage. The data, expressed in terms of moles CO_2 per mole AMP (α) at a specified partial pressure (kPa), are shown in Table 1 and plotted in Figure 3. The results are in good agreement with the previous study.

Table 1.

Solubility of CO_2 in 3.0 M Aqueous AMP at 40°C

α (mol CO_2 / mol AMP)	P (kPa)
0.404	1.25
0.564	2.79
0.604	3.54
0.728	12.8
0.769	19.0
0.786	15.6
0.818	22.5
0.835	36.6
0.919	99.5
0.948	144.
0.960	359.
0.982	216.

Complex phase behaviour was observed during the preliminary study of the solubility of CO_2 in mixed AMP solutions. A white solid phase formed in solutions of high sulfolane or AMP concentrations. Several solutions with varying amounts of AMP and sulfolane were tested for this

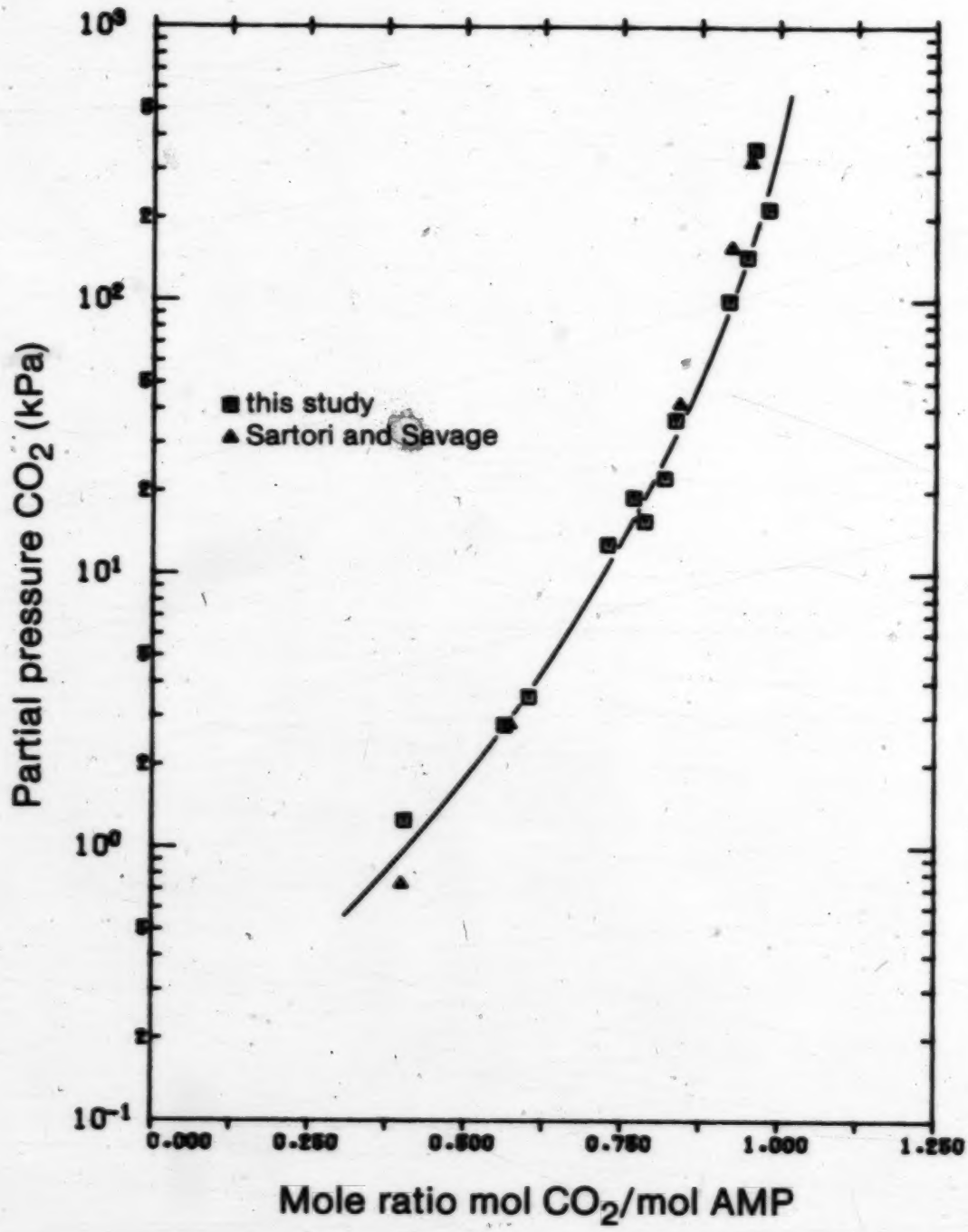

Figure 3 Solubility of CO_2 in 3.0 M aqueous AMP at 40°C

formation at 40°C and a partial pressure of 5500 kPa. The results are shown in Table 2.

Table 2.

Solid Formation in Mixed Solvent at 40°C and 5500 kPa

AMP molarity	weight % AMP	weight % sulfolane	phases observed
1.50	11.6	65.8	solid/liquid
1.50	12.8	19.9	liquid
1.50	12.2	43.9	liquid
1.55	12.4	49.0	solid/liquid
2.00	16.5	32.2	liquid
2.06	17.0	36.7	solid/liquid
2.25	18.8	29.2	liquid
2.58	21.7	31.4	solid/liquid
3.00	24.4	37.8	solid/liquid
3.00	25.4	24.8	solid/liquid

Heating the solution to 70°C caused the solid phase to disappear. The solid was relatively stable and could be removed from the equilibrium cell and kept at room conditions for several minutes. The solid phase was soluble in water and addition of aqueous $BaCl_2$ to this solution yielded a precipitate indicating the presence of carbonate. Titration of the filtrate with HCl indicated the presence of AMP. The solid phase was only slightly soluble in sulfolane.

These observations may be explained by considering the solid to be an amine carbonate salt. The salt is soluble in aqueous systems but is less soluble as the sulfolane is added. From this it follows that the possibility of solid formation would increase as the concentration of the amine or CO_2 loading increases and the water content decreases.

This is in accordance with the experimental observations.

Based upon these preliminary results, a mixed solution of 16.5 wt % AMP (2.0 M), 32.2% sulfolane and 51.3% water was selected for the solubility study.

4.2 Experimental Results

The equilibrium solubility of CO_2 and H_2S was measured in the mixed solvent, in a 2.0 M aqueous AMP solution, and in sulfolane at 40 and 100°C. The solubility of H_2S in the mixed solvent at 40°C could be determined only to approximately 1600 kPa. A second liquid phase formed at higher H_2S partial pressures. The results for the mixed and aqueous solvents are expressed in terms of moles acid gas absorbed per mole AMP (α). The results for the solubility in sulfolane are expressed in mole fraction acid gas in the liquid. The data are shown in Tables 3 to 8.

As the mixed and aqueous solvent have the same concentration of AMP, the influence of the physical solvent can be assessed by a direct comparison of the solubility curves which are shown in Figures 4 and 5. The solubility of CO_2 and H_2S at 40°C is significantly lower in the mixed solvent than in the aqueous solvent at acid gas partial pressures less than 10 kPa. As the partial pressure increases, the difference in the solubility decreases until at a loading of approximately 1 mol/mol AMP, the solubilities are essentially identical. At higher partial pressures, the solubility is greater in the mixed solvent.

Table 3

Solubility of CO_2 at 40 °C and 100 °C in 2.0 M Aqueous AMP

40 °C		100 °C	
α	P (kPa)	α	P (kPa)
0.493	2.17	0.136	8.53
0.732	9.58	0.193	16.2
0.742	10.6	0.292	35.3
0.916	44.5	0.414	73.2
0.952	95.4	0.583	172.
1.008	266.	0.776	466.
1.042	640.	0.832	551.
1.059	653.	0.896	886.
1.084	1140.	0.998	1330.
1.128	1800.	1.033	1960.
1.190	2680.	1.162	3530.
1.325	5740.	1.275	5870.

Table 4

Solubility of CO_2 at 40 °C and 100 °C in 2.0 M Mixed Solvent

40 °C		100 °C	
α	P (kPa)	α	P (kPa)
0.397	2.63	0.0634	8.70
0.542	5.34	0.133	29.5
0.615	9.14	0.204	58.9
0.790	28.4	0.293	112.
0.920	79.9	0.383	200.
0.961	175.	0.513	358.
1.043	478.	0.611	760.
1.045	394.	0.828	1560.
1.091	928.	0.984	2240.
1.120	942.	1.133	3620.
1.125	1150.	1.270	6050.
1.172	1830.		
1.194	2100.		
1.252	2500.		
1.270	2660.		
1.300	3390.		
1.367	3610.		
1.393	4050.		
1.440	5740.		
1.476	4730.		
1.610	6110.		
1.621	5630.		

Table 5

Solubility of H_2S at 40 °C and 100 °C in 2.0 M Aqueous AMP

40 °C		100 °C	
α	P (kPa)	α	P (kPa)
0.618	2.69	0.140	2.26
0.630	2.93	0.203	5.51
0.726	5.46	0.256	9.40
0.793	9.79	0.400	23.9
0.794	8.82	0.506	31.8
0.834	13.1	0.529	51.8
0.904	30.3	0.750	148.
0.970	68.8	0.786	187.
1.021	178.	0.979	466.
1.109	380.	1.126	947.
1.175	566.	1.278	1580.
1.253	797.	1.405	2010.
1.441	1280.		
1.495	1470.		
1.715	2160.		

Table 6

Solubility of H_2S at 40 °C and 100 °C in 2.0 M Mixed Solvent

40 °C		100 °C	
α	P (kPa)	α	P (kPa)
0.488	2.45	0.0979	4.54
0.611	7.06	0.121	6.21
0.660	7.09	0.218	16.2
0.831	22.1	0.357	45.1
0.896	35.3	0.531	110.
0.941	55.1	0.694	229.
0.985	92.0	0.946	515.
1.052	180.	1.092	809.
1.182	346.	1.254	1200.
1.325	565.	1.378	1500.
1.474	775.	1.636	2200.
1.696	1120.		
1.917	1390.		
2.152	1610.		

Table 7

Solubility of CO_2 at 40 °C and 100 °C in Sulfolane

40 °C		100 °C	
x	P (kPa)	x	P (kPa)
0.00971	105.	0.0104	249.
0.00985	103.	0.0171	444.
0.0177	185.	0.0298	731.
0.0261	278.	0.0574	1520.
0.0329	377.	0.0867	2360.
0.0966	1080.	0.160	4690.
0.136	1610.	0.197	5900.
0.218	2530.		
0.268	3520.		
0.330	4140.		
0.420	5580.		

Table 8

Solubility of H_2S at 40 °C and 100 °C in Sulfolane

40 °C		100 °C	
x	P (kPa)	x	P (kPa)
0.0451	123.	0.0527	348.
0.108	261.	0.0974	720.
0.198	519.	0.142	1040.
0.293	761.	0.183	1270.
0.368	981.	0.219	1580.
0.453	1240.	0.309	2350.
0.549	1600.		
0.702	2090.		

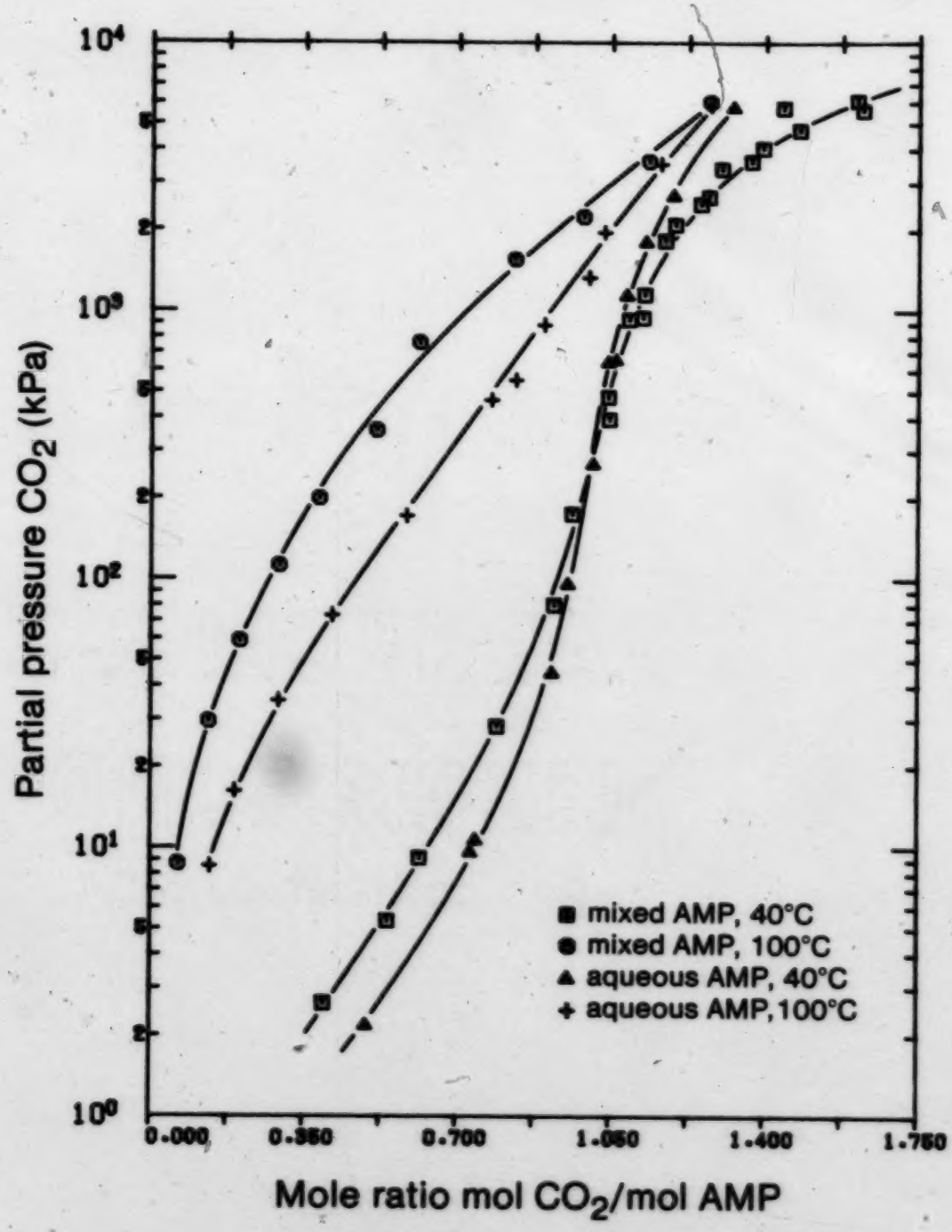

Figure 4 Solubility of CO_2 in mixed and aqueous AMP.

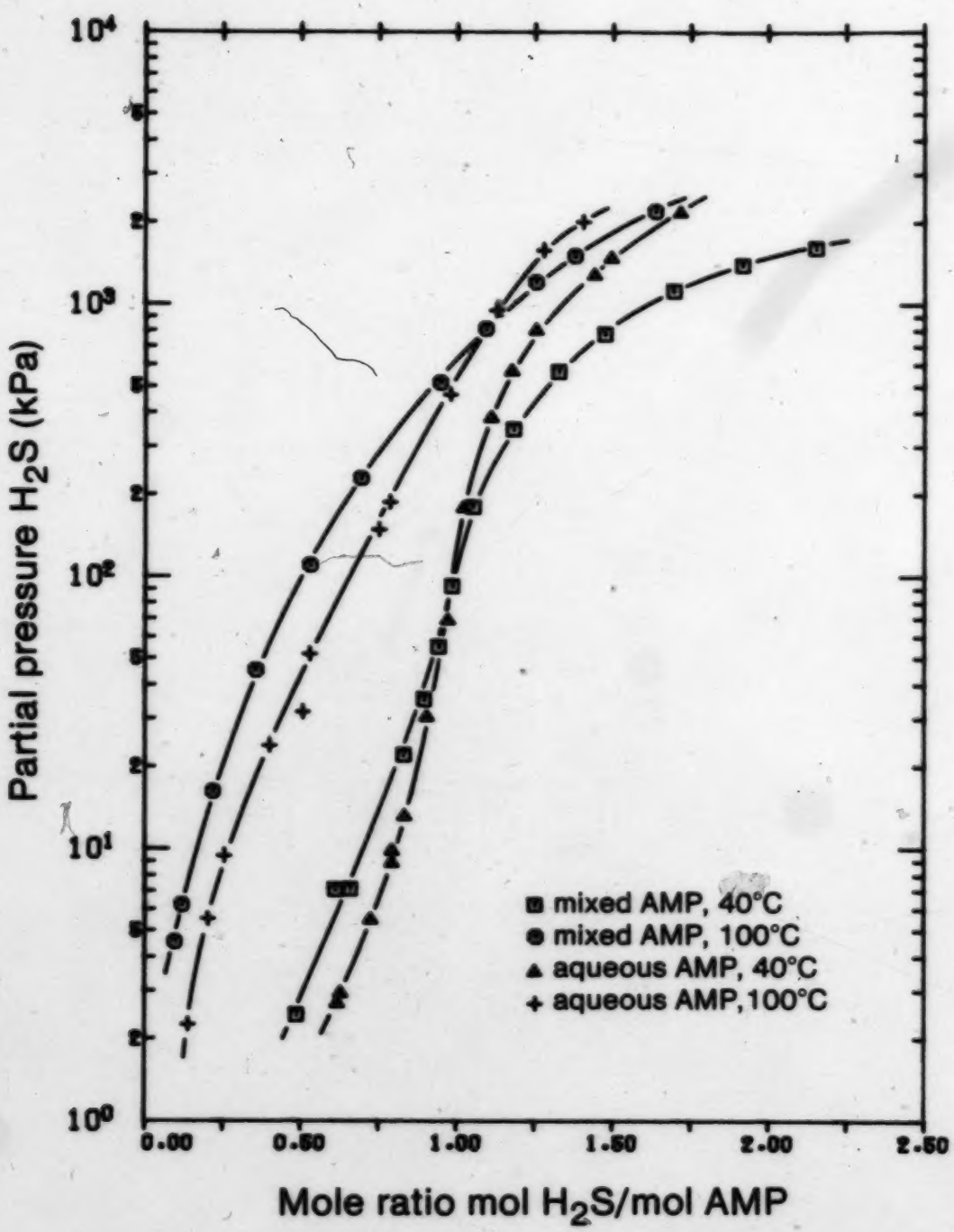

Figure 5 Solubility of H_2S in mixed and aqueous AMP.

The difference in solubility is more pronounced for H_2S than CO_2.

At 100°C the solubility of CO_2 and H_2S is similarly lower in the mixed solvent at low partial pressures. Higher partial pressures and liquid loading, however, are required at 100°C to attain the point at which the solubilities in the two solvents are equal.

The data for the solubility of CO_2 and H_2S in sulfolane at 40 and 100°C are plotted in Figures 6 and 7. The relationship between partial pressure and mole fraction is linear at dilute concentrations and becomes nonlinear at higher liquid concentrations. Henry's constants for each system were calculated by linear regression analysis of the variation of vapour fugacity with mole fraction. The values are compared with those reported by Rivas (in parentheses) in Table 9.

Table 9

Henry's Constants for CO_2 and H_2S in Sulfolane

	40°C	100°C
H_{CO_2} (MPa)	10.4 (11.3)	25.8 (25.1)
H_{H_2S} (MPa)	2.49 (2.56)	6.80 (6.33)

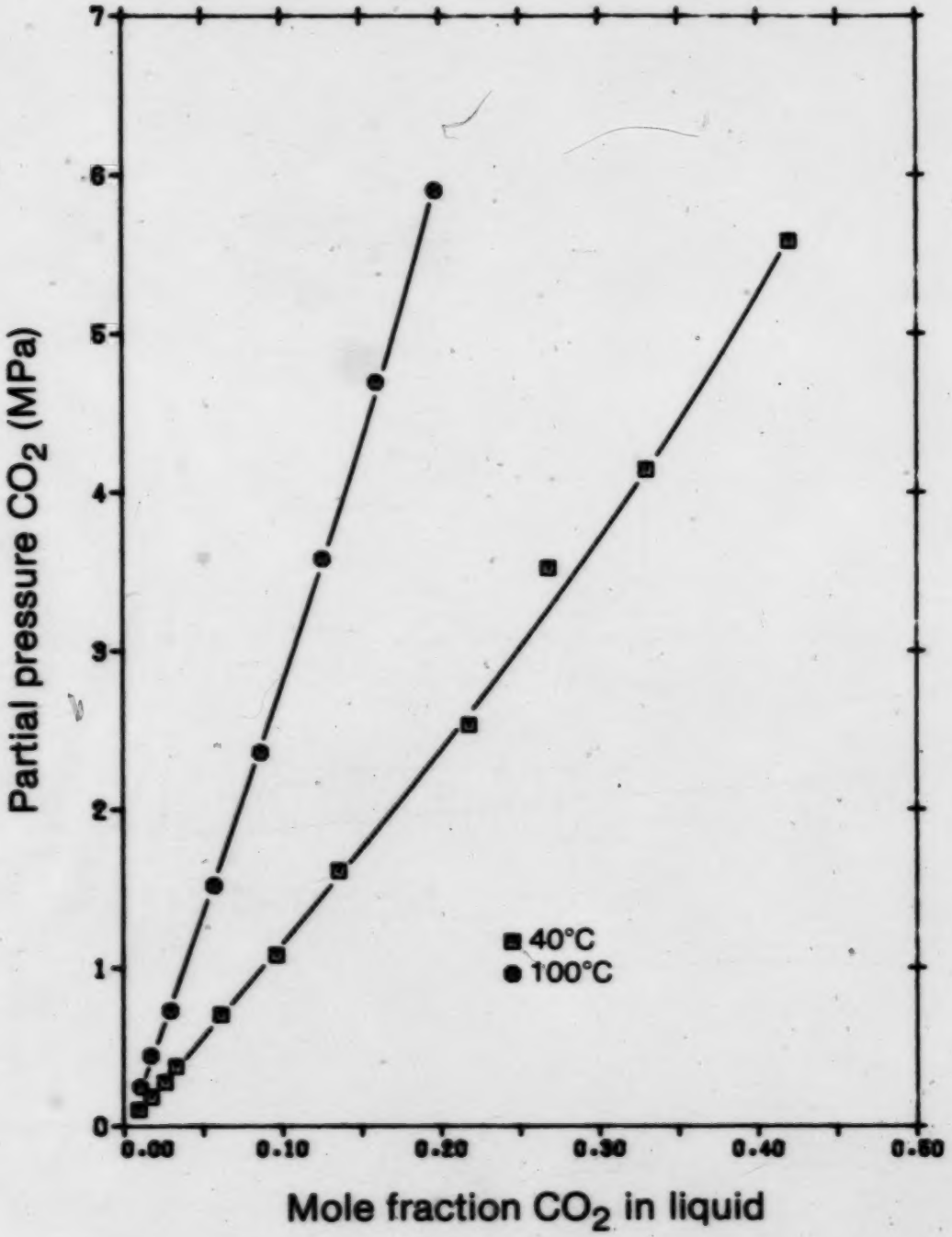

Figure 6 Solubility of CO_2 in sulfolane.

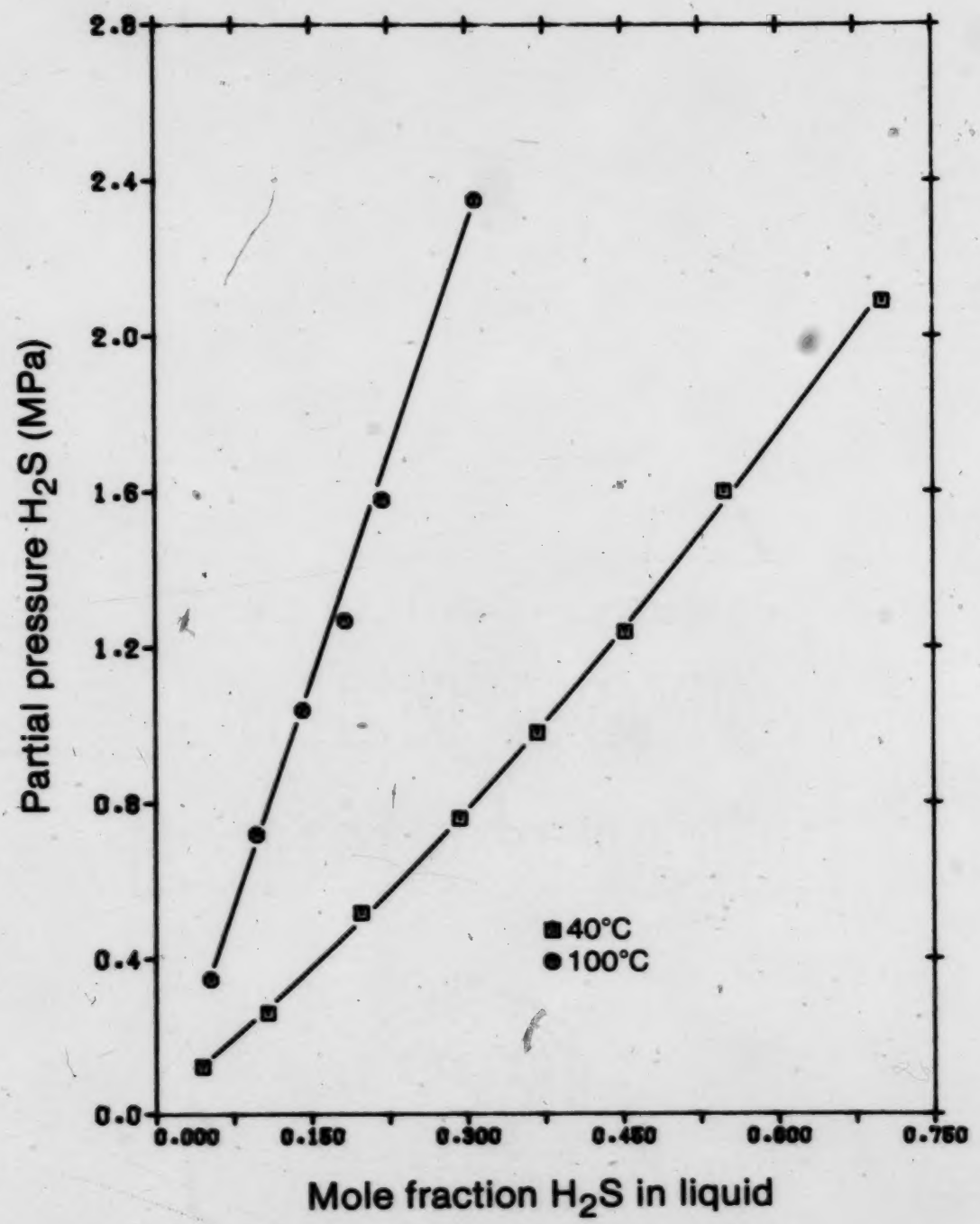

Figure 7 Solubility of H_2S in sulfolane.

4.3 Accuracy of Data

The measured quantities which influence the accuracy of the data are the acid gas content of the liquid sample, the amine solution concentration and density, the vapour phase mole fraction, and the total system pressure. The uncertainty in each of these quantities may in turn be affected by other measurements. For example, the uncertainty in the vapour phase composition is influenced by the accuracy of the response factor measurement. The overall error was estimated from the individual uncertainties by a Taylor series expansion:

$$\Delta X = \sum_i \left(\frac{\partial X}{\partial Y_i}\right) \Delta Y_i \qquad (4.1)$$

Details of the error analysis are outlined in Appendix 4.

The error in the solution loading is estimated at ± 2 to 3% in the range studied. This error arises principally from the determination of the acid gas and amine content of the liquid sample. The uncertainty in the partial pressure decreases as the pressure increases and ranges from ±11% at 5 kPa to ±0.4% at 6 000 kPa. At low pressure, the error in the vapour phase analysis is the most important factor. At higher pressures, the sensitive measurement becomes that of the total pressure.

4.4 Discussion of Experimental Results

The replacement of water with sulfolane has two opposing influences on the solubility behaviour. At high partial pressures, the presence of the physical solvent increases the capacity for the acid gases. At low pressure, the effect is reversed, and the solubility in the mixed solvent is reduced by the physical solvent component. A rationalization of these results may be best accomplished by focussing on each influence separately.

As noted previously, as α approaches 1 mol/mol AMP, the free amine concentration decreases rapidly, and the proportion of acid gas in the molecular form increases. This increase in the molecular concentration is reflected in the rise in partial pressure of the acid gas over the solution. As the solution is further loaded, the absorption becomes similar to that of strictly physical solvents. From Equation (2.4), a plot of vapour fugacity versus liquid molality should be approximately linear. A plot of this type, shown in Figure 8, is based on the data for the solubility of H_2S in mixed and aqueous solvents. The molality has been estimated by assuming that all the H_2S less than 1 mol/mol AMP exists as the ionic species, and that the H_2S absorbed beyond this point does not dissociate. A linear relationship is observed and the slope of these lines may be considered to be approximate values for the Henry's constant in the solvent. As anticipated, the physical solubility in the mixed solvent is greater than the corresponding aqueous

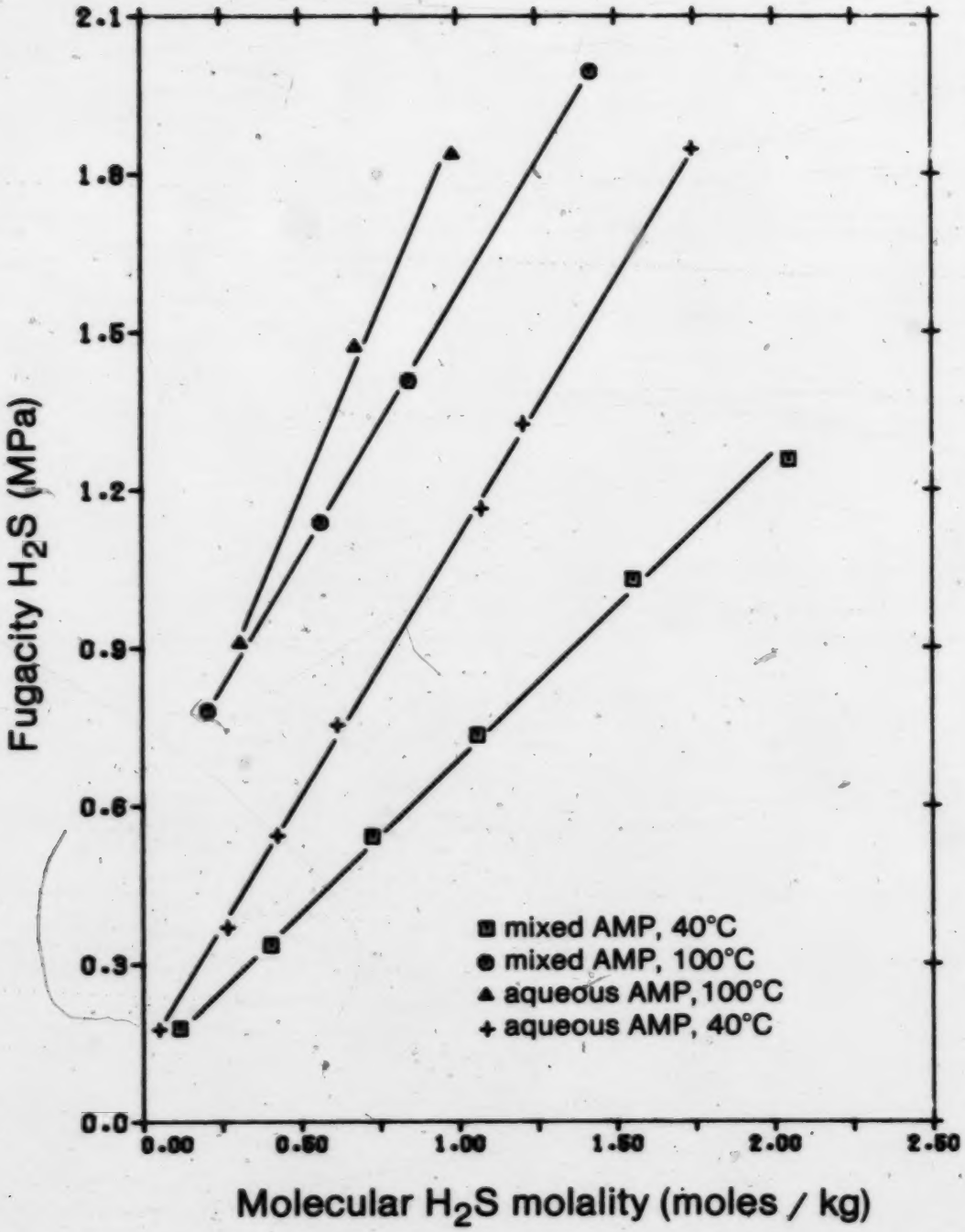

Figure 8 Physical solubility of H_2S in mixed and aqueous AMP.

solvent.

Given the higher physical solubility for the mixed solvent, an opposing influence of the sulfolane component must be in effect at lower loadings. Under these conditions, the solvent contains, at a set liquid loading, a higher proportion of the molecular form. Thus, the replacement of a portion of the water has altered the chemical equilibria between the reacting species in the liquid.

Solvent effects on ionic processes have recently been reviewed by Sen et al. (1982) who rationalized these effects using the Born electrostatic model. According to this model, the pKa varies inversely with the dielectric constant of the solvent. The dielectric constants of pure sulfolane and water at 40°C are 42.1 and 73.1 respectively. Therefore, as the dielectric constant of the mixed solvent is lower than the aqueous solvent, the dissociation of CO_2 and H_2S is reduced.

5. CORRELATION OF EXPERIMENTAL DATA

A numerical model for correlating the solubility data for the aqueous and mixed solvents has several applications. A model provides a means to interpolate between experimental points within the solubility range studied and to extrapolate beyond this range where data are not available. A model which accurately predicts the experimental results may be suitable to estimate the solubility at other temperatures, or amine concentrations, or to predict the solubility of mixtures of CO_2 and H_2S. A numerical model with these capabilities is a necessary component of computer simulation programs for amine treating units (Tomcej et al., 1983).

5.1 Survey of Models

The equations which must be solved to calculate the vapour and liquid compositions are outlined in Appendix 5. The equations describe the physical vapour-liquid equilibria for the volatile molecular components, the chemical equilibria between the reacting species, and the stoichiometric relationships between the liquid phase components. A rigourous solution requires a knowledge of the chemical equilibrium constants, the Henry's constants, and a method to determine the vapour phase fugacity coefficients and the liquid phase activity coefficients.

The models which have been proposed for the acid gas/amine system and the analogous NH_3-CO_2-H_2S-H_2O system

generally differ in the treatment of the vapour and liquid nonidealities. Van Krevelen et al. (1949) assumed an ideal solution in the liquid phase and ideal gas in the vapour phase to simplify the set of equations. Empirical expressions for the equilibrium constants as a function of temperature and ionic strength were used. Kent and Eisenberg (1975) also neglected liquid and vapour nonidealities in their correlation of the solubility of acid gases in aqueous amines. The equilibrium constants for the dissociation of the amine and for the carbamate formation were treated as adjustable parameters and determined by a best fit of the experimental data.

A method for introducing activity coefficients was first proposed by Atwood et al. (1957) and generalized by Klyamer et al. (1973). Activity coefficients of the ionic species were assumed to be equal and functions only of ionic strength. The relationship between the activity coefficient and the ionic strength was obtained by fitting the data for the H_2S - amine - water system. The model sets the activity coefficient of free H_2S and CO_2 to unity and neglects nonidealities in the gas phase.

Edwards et al. (1975) proposed a more accurate representation of the liquid phase nonidealities in the development of a model for the NH_3-H_2S-CO_2-H_2O system. The activity coefficient of the liquid phase species is given by a form of the extended Debye-Hückel law:

$$\ln \gamma_i = \frac{-A\, z_i^2 \sqrt{I}}{1 + b\sqrt{I}} + 2 \sum_{j \neq w} \beta_{ij} \qquad (5.1)$$

The first term accounts for the electrostatic forces as derived from the Debye-Hückel theory. The second term expresses the short range (Van der Waals) interactions between the solute species and incorporates an empirical interaction coefficient, β.

This approach was applied by Deshmukh and Mather (1981) for a correlation of the solubility of acid gases in aqueous amine solutions. Coefficients for the interaction between dominant species were estimated by a best fit of the experimental data and were assumed to be independent of composition or temperature. Vapour phase fugacity coefficients were estimated by an equation derived from the Peng-Robinson equation of state.

More accurate expressions for the activity coefficients have been recently proposed and attempt to account for the interactions between the liquid phase species. Edwards et al. (1978) used a form of an equation derived by Pitzer (1973) to account for binary interactions of all types: ion-ion, molecule-molecule, and ion-molecule. Beutier and Renon (1978) used the Pitzer equation to determine the contribution to the excess Gibbs free energy arising from ion-ion interactions. Molecule-molecule interactions are

described by a Margules type expression while molecule-ion forces are estimated from equations based upon the Debye-McAulay theory. Chen et al. (1979) applied an expression similar in form to that derived by Pitzer to account for the influence of molecular solutes in solution.

The accuracy, range of application, and ease of use differ widely among the models described above. Owing to their neglect of vapour phase fugacity coefficients and their simple treatment of the liquid nonidealities, the Kent and Eisenberg and Klyamer et al. models are restricted to solution loading less than 0.7 mol/mol amine. The models of Edwards et al. (1975) and Deshmukh and Mather provide a more accurate representation of the thermodynamics, but become more difficult to use as they require the estimation of binary interaction parameters. The incorporation of more complex expressions for the activity coefficients (Edwards et al., 1978, Beutier and Renon, Chen et al.) increases the accuracy further, but requires the estimation of even more parameters.

The correlation of the solubilty of CO_2 and H_2S in mixed and aqueous AMP solutions was based on the model developed by Deshmukh and Mather. The modifications to the model and the results of the correlation are outlined in the following sections.

5.2 Correlation of Acid Gas Solubility in Aqueous AMP

The model as originally developed by Deshmukh and Mather has been sucessfully applied to aqueous solutions of MEA, DEA, and DIPA at amine concentrations to 5 M and temperatures to 100°C. Two major modifications were required to apply the model to the aqueous AMP system. The chemical equilibrium expression for the formation of the carbamate species was deleted from the set of equations. As noted previously, this reaction is destabilized by the presence of the bulky substituent group (Sartori and Savage, 1983). A second modification to the original method is required to specify the dissociation constant for AMP. In the original model, the values for the chemical equilibrium constants and Henry's constants were obtained from the literature. The dissociation constant for AMP, however, is not well known over the temperature range of interest. Instead, the dissociation constant in the aqueous system at 40 and 100°C was estimated from the experimental solubility at the lowest loading examined where the liquid nonidealities would be a minimum. The equations were solved for the dissociation constant with the interaction coefficients set to 0. The estimated pKa values were 9.46 and 7.97 at 40 and 100°C.

A computer program was used to determine the interaction coefficients which minimized the sum of the squared deviations between the experimental and predicted partial pressures at solution loadings less than 1 mol/mol AMP. Adjustment of the interaction parameters did not

influence the predictions above a loading of 1 mol/mol AMP. As in the original model, only the interactions between the dominant species were considered. The interactions considered are: HS^--RNH_3^+, HS^--RNH_2, HCO_3^--RNH_3^+, HCO_3^--RNH_2. The interaction coefficients determined from the CO_2 and H_2S solubility data are:

$$\beta_{HCO_3^- - RNH_3^+} = 0.0427 \qquad \beta_{HCO_3^- - RNH_2} = 0.260$$

$$\beta_{HS^- - RNH_3^+} = 0.0518 \qquad \beta_{HS^- - RNH_2} = -0.0348$$

The remaining chemical equilibrium constants and Henry's constants were obtained from the literature. The first and second ionization constants for H_2S were given by expressions reported by Barbero et al. (1982) and Kryukov et al. (1974) respectively. Similar expressions for the first and second ionization constants of CO_2 were given by Patterson et al. (1982) and Kent and Eisenberg (1975). The Henry's constants for CO_2 and H_2S were given by equations reported by Mason and Kao (1980) and Lee and Mather (1978).

The predicted acid gas solubility is compared with the experimental values in Figures 9 and 10. The predicted solubility agree closely with the experimental results at solution loadings less than 1 mol/mol AMP. At higher loadings, the predicted solubility deviates significantly from the experimental values.

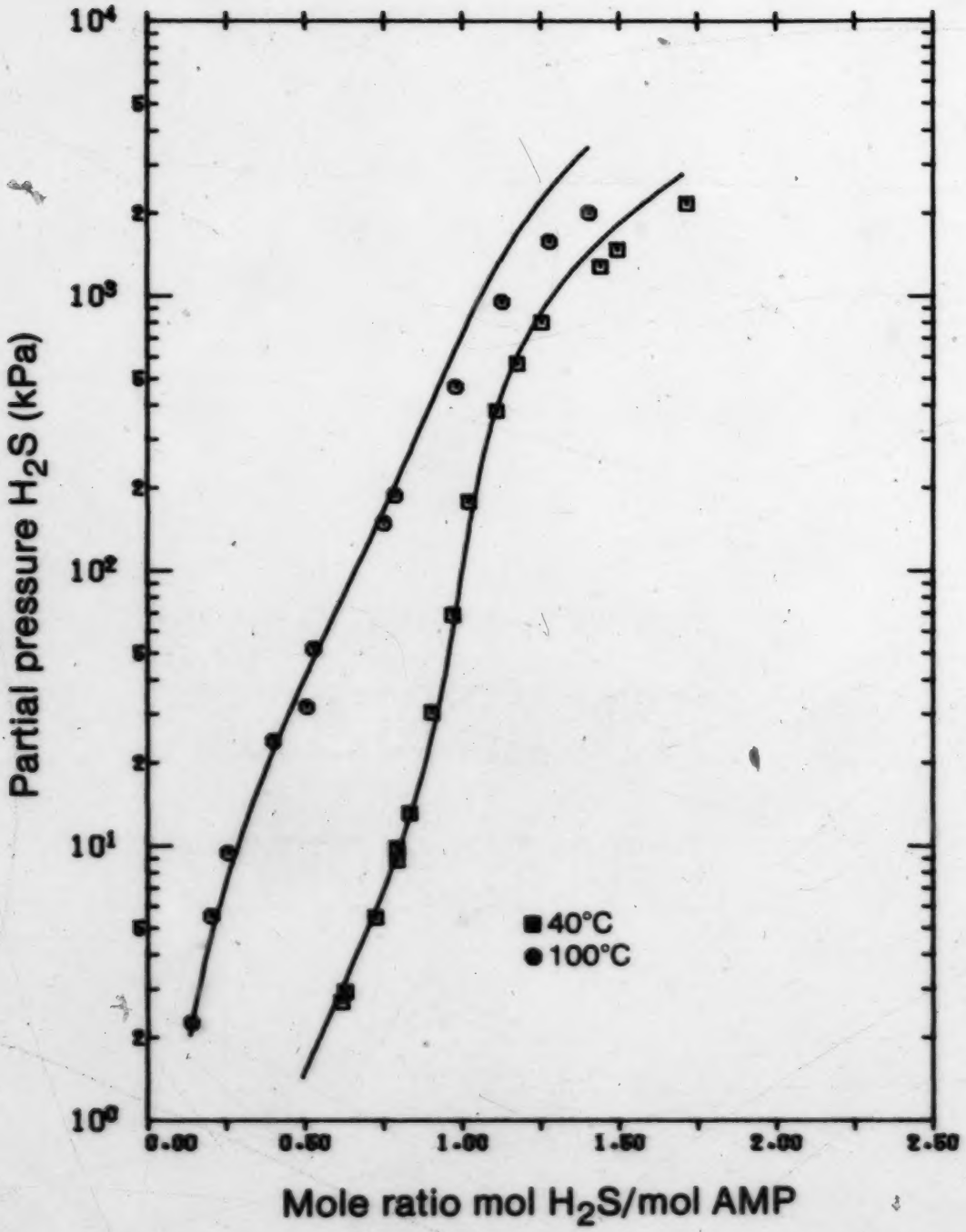

Figure 9 Comparison of predicted and experimental H_2S solubility in aqueous AMP.

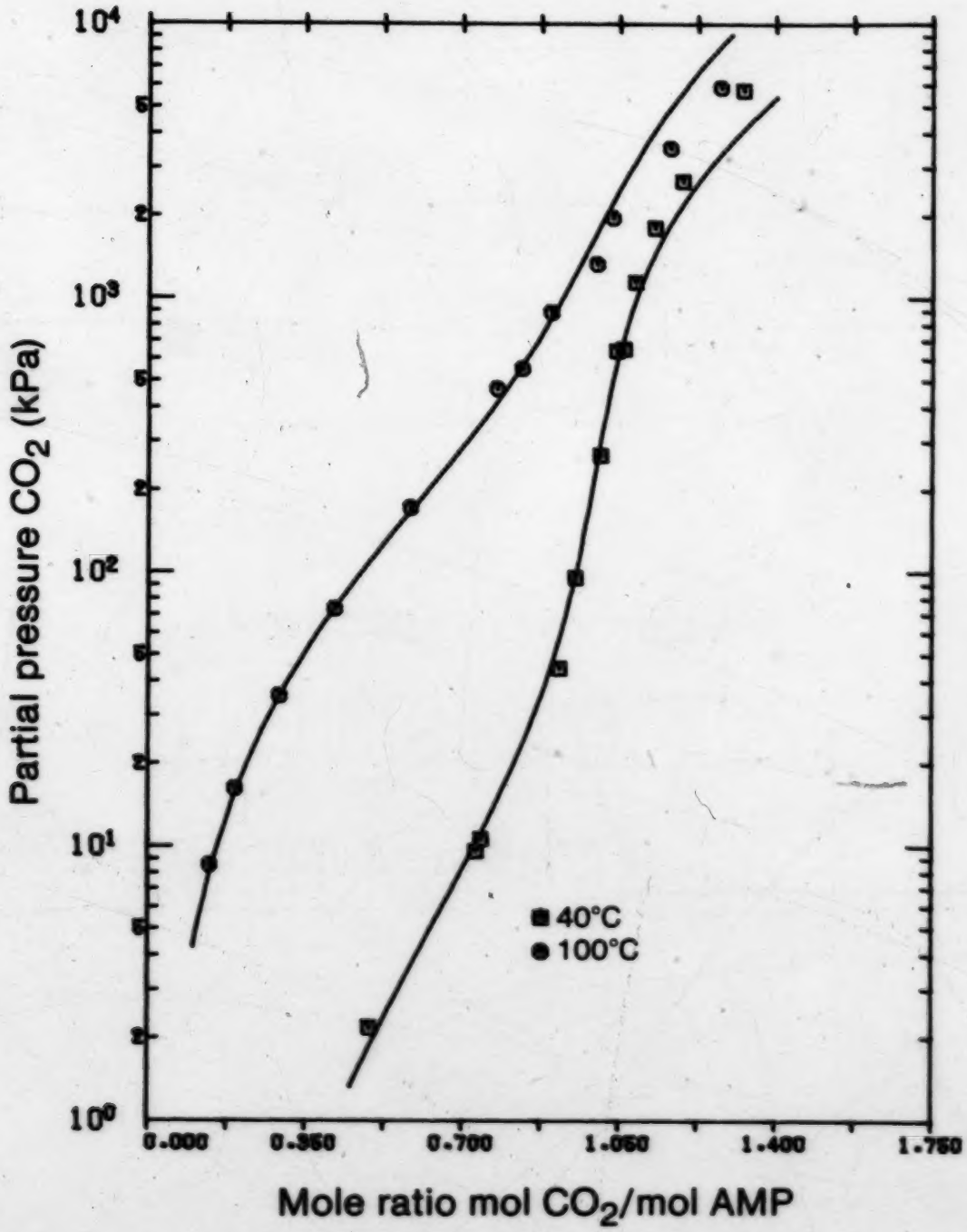

Figure 10 Comparison of predicted and experimental CO_2 solubility in aqueous AMP.

5.3 Correlation of Solubility in Mixed AMP

The interaction coefficients are assumed to be independent of solvent composition. Thus, the interaction coefficients for the mixed solvent system have been set equal to the values estimated in the correlation of the aqueous AMP. The solvent composition, however, has a strong influence on the values for the chemical equilibrium constants and the Henry's constants. The use of these constants as obtained from the literature for strictly aqueous systems is inappropriate. The method of Deshmukh and Mather must therefore be modified to account for the solvent effects.

Several methods have been proposed for estimating Henry's constants in mixed solvents. Generalized methods have been based on the solubility parameter theory (Hildebrand et al., 1970), the Kirkwood-Buff solution theory (O'Connell, 1971) and a simplified form of perturbation theory (Tiepel and Gubbins, 1972). O'Connell (1971) derived expressions for the Henry's constant by considering various models for the excess Gibbs free energy such as the Margules equation, the Wilson equation, and the Van Laar equation. The methods, which generally require the knowledge of the Henry's constants in the pure solvent and the estimation of various parameters, have not been applied to a chemically reactive solvent. Rivas estimated the Henry's constant in nonaqueous amine-organic sovents by an equation proposed by O'Connell and Prausnitz (1961).

$$\ln H_{1m} = x_2 \ln H_{12} + x_3 \ln H_{13} - \frac{A_{23}\, x_2\, x_3}{RT} \qquad (5.2)$$

H_{12}, the Henry's constant in the amine, was estimated by a correlation of Prausnitz and Shair (1961).

The methods outlined above are difficult to apply to the ternary AMP-water-sulfolane system as they require the knowledge of the Henry's constant in the amine and various mixture parameters. The estimation of the Henry's constant has been simplifed in this study by using the experimental data at high solution loading where chemical reactions becomes less significant. As noted previously and shown in Figure 8, the relationship between the fugacity of the acid gas and the liquid molality of the free species is linear. An estimation of the Henry's constant in the mixed solvent was obtained by linear regression analysis.

The chemical equilibrium constants will differ from those for the aqueous system due to the reduction in the dielectric constant. The solvent effect on the chemical equilibrium constant has been considered only for the dominant reactions:

$$RNH_3^+ = RNH_2 + H^+ \qquad (5.3)$$

$$H_2S = HS^- + H^+ \qquad (5.4)$$

$$CO_2 + H_2O = HCO_3^- + H^+ \qquad (5.5)$$

$$HCO_3^- = CO_3^{-2} + H^+ \qquad (5.6)$$

The equilibrium constants for the dissociation of AMP and H_2S were estimated at 40 and 100°C by a best fit of the experimental data for the solubility of H_2S in the mixed solvent. Equilibrium constants for the formation of bicarbonate and carbonate ions were estimated in a similar manner from the data of CO_2 solubility. The estimated values for the Henry's constants and chemical equilibrium constants are shown in Table 10. All other equilibrium constants are as used for the aqueous system. The predicted acid gas solubility is compared with the experimental values in Figures 11 and 12. An excellent agreement between predicted and experimental solubility is observed. The deviation at loadings greater than 1 mol/mol AMP is less that obtained for the correlation of the solubility in the aqueous AMP solvent.

5.4 Predictive Application of Solubility Model

A knowledge of the chemical equilibrium constants and Henry's constants at temperatures between 40 and 100°C enables the solubility in this temperature range to be estimated. The constants were estimated by the application of the van't Hoff equation.

$$\frac{\partial \ln K}{\partial T} = \frac{\Delta H^\circ}{R T^2} \qquad (5.7)$$

K may represent either the chemical equilibrium constant or the Henry's constant. If ΔH° is assumed to be independent of

Table 10

Henry's constants and chemical equilibrium constants in mixed AMP at 40 and 100°C

		40°C	100°C
H_{CO_2}	(MPa kg/mol)	3.92	5.98
H_{H_2S}	(MPa kg/mol)	0.667	1.35
pK_1		8.92	7.21
pK_2		6.99	6.69
pK_3		6.35	6.49
pK_4		10.58	10.41

Reactions:

1. $RNH_3^+ = RNH_2 + H^+$
2. $H_2S = HS^- + H^+$
3. $CO_2 + H_2O = HCO_3^- + H^+$
4. $HCO_3^- = CO_3^{-2} + H^+$

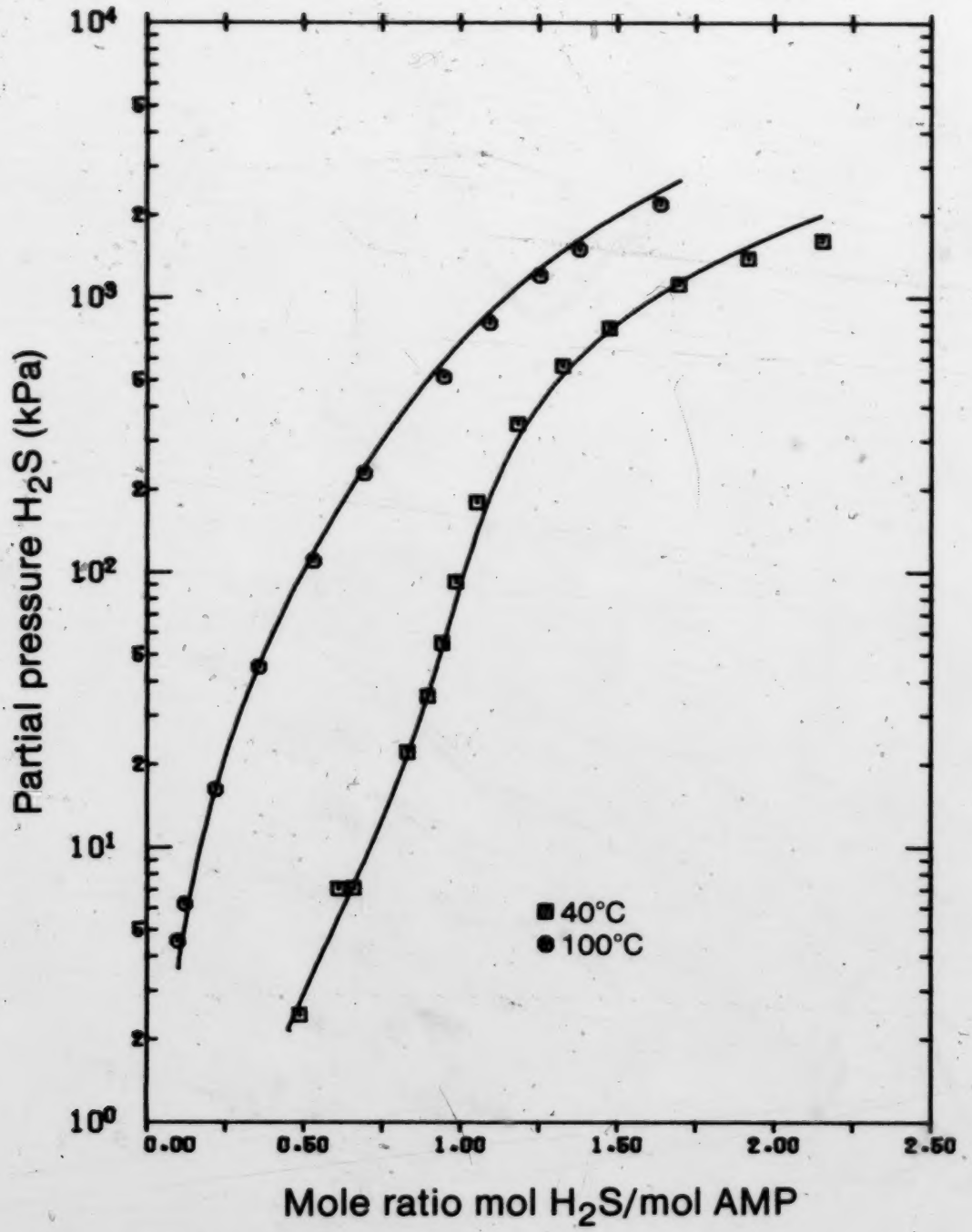

Figure 11 Comparison of predicted and experimental H_2S solubility in mixed AMP.

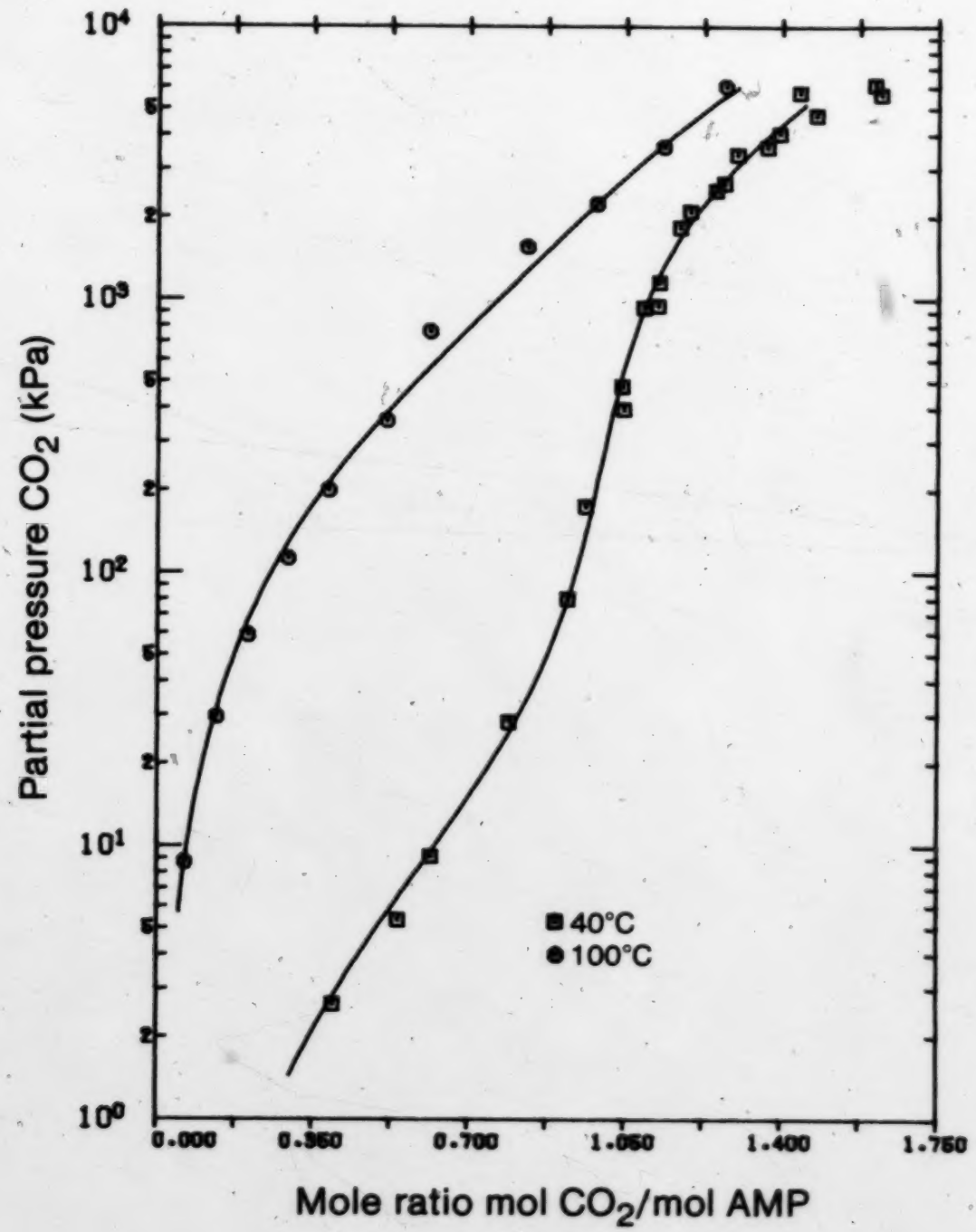

Figure 12 Comparison of predicted and experimental CO_2 solubility in mixed AMP.

temperature over the range of interest, Equation (5.7) may be integrated to yield:

$$\ln K = I - \frac{\Delta H^{\circ}}{R T} \qquad (5.8)$$

By knowing K at two temperatures, I and ΔH° may be evaluated.

The solubility of H_2S at various temperatures in the 2.0 M mixed AMP solution is shown in Figure 13.

A second application of the model is the prediction of the solubility of mixtures of CO_2 and H_2S over the amine solution. The effect of CO_2 loading on the solubility of H_2S in the 2.0 M mixed AMP solution at 40°C is shown in Figure 14.

5.5 Discussion of Correlative Model

The improved agreement between predicted and experimental results for the mixed solvent over the aqueous solvent at high loading is attributed to the method of the determination of the Henry's constant. The Henry's constants for the aqueous AMP solution were the literature values as evaluated from the experimental solubility of CO_2 and H_2S in pure water. It is therefore expected that these values would differ from the Henry's constant in a mixture of water and amine. Adjustment of the interaction parameters may account for the inaccuracy in the Henry's constant at low loading, but would have less influence at higher loadings of the acid

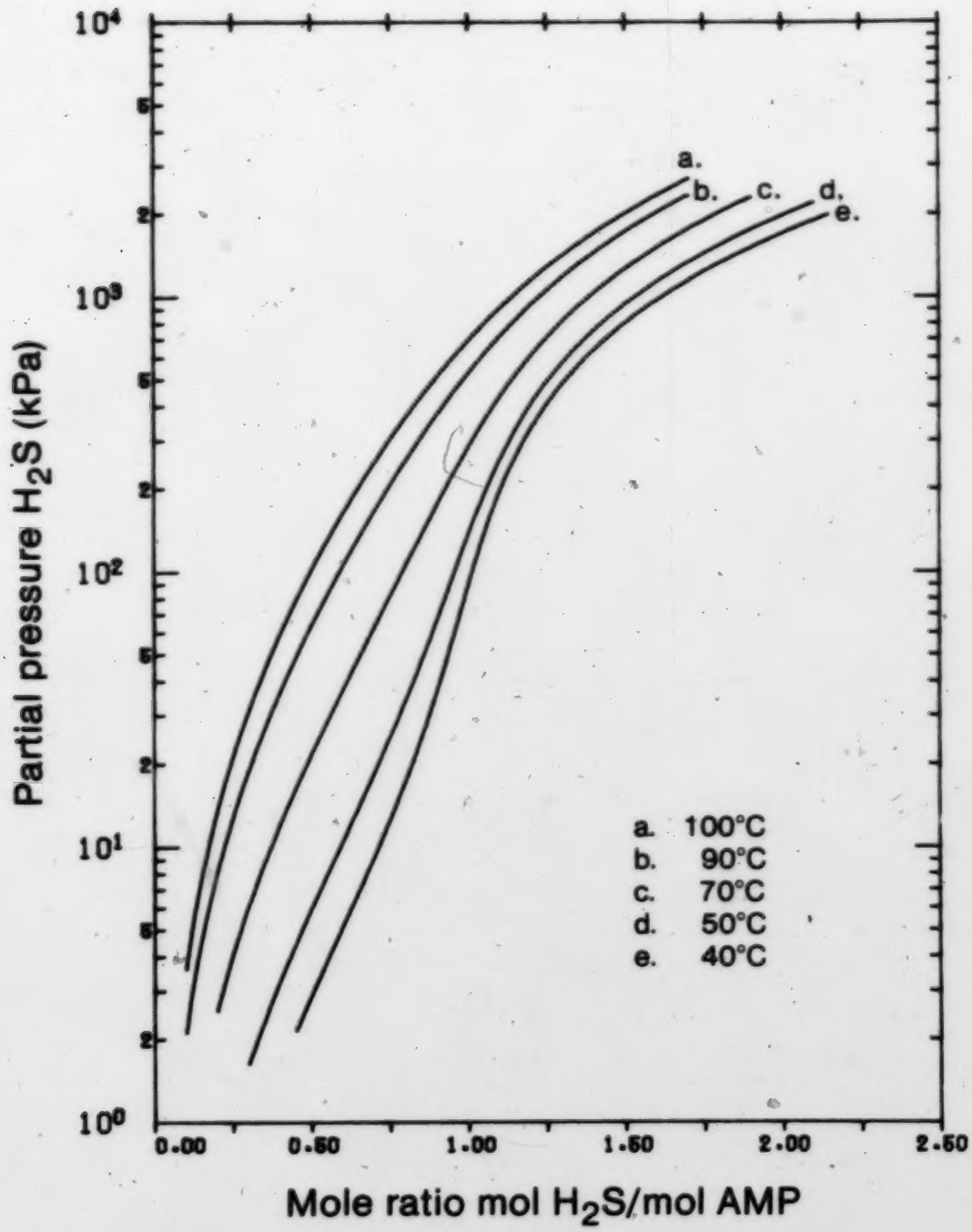

Figure 13 Predicted effect of temperature on solubility of H_2S in mixed AMP.

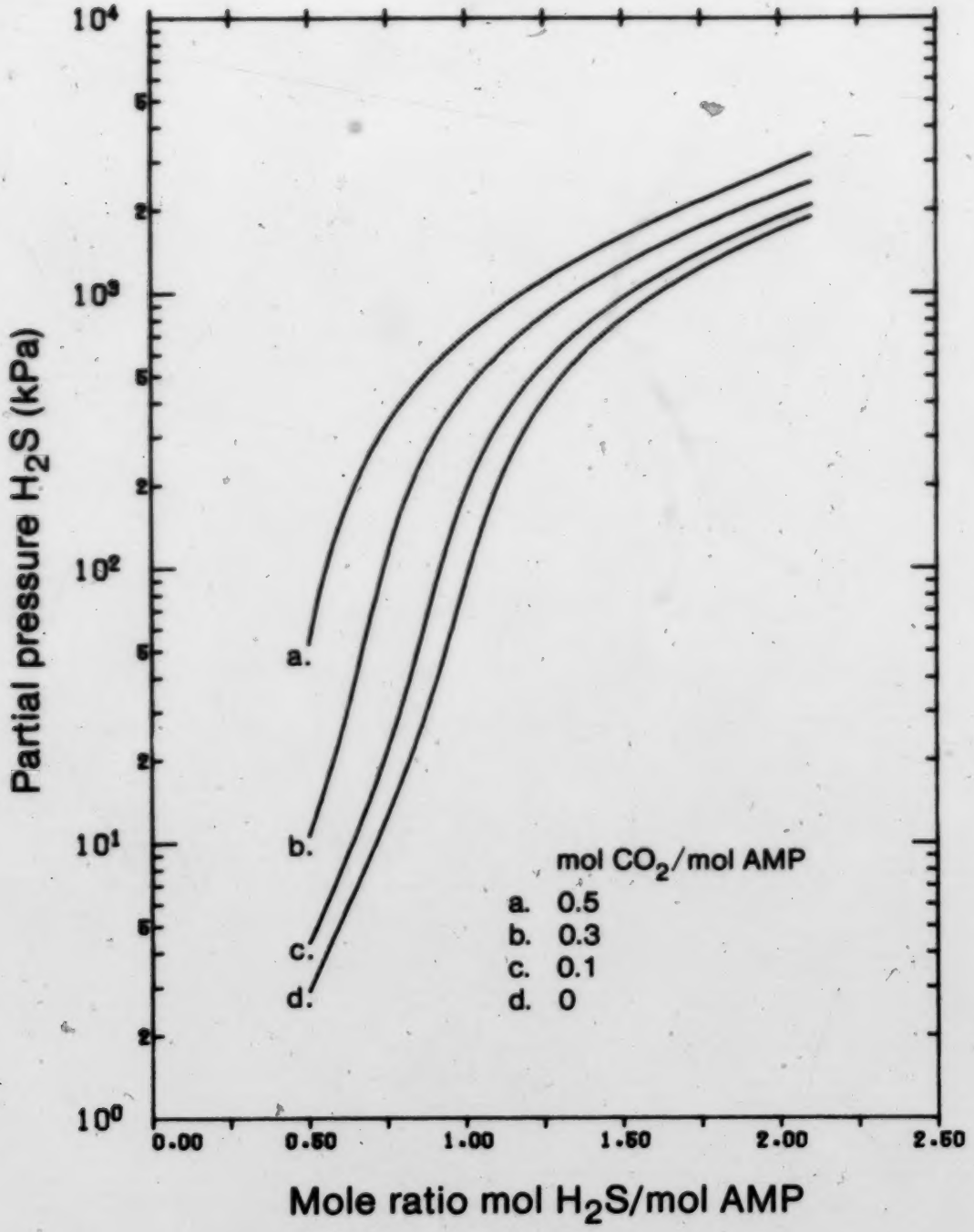

Figure 14 Predicted effect of CO_2 loading on solubility of H_2S in mixed AMP solution at 40°C.

gas. The inaccuracy of the Henry's constant leads to the significant deviation between predicted and experimental values in the aqueous solvent at solution loadings greater than 1 mol/mol AMP.

Solvent effects on the chemical equilibria have been considered only for the dominant reactions. The solvent composition, however, will influence all liquid phase reactions. For example, the dissociation constant for water has been measured in several organic solvents (Woolley et al., 1970). The influence of the solvent on the chemical equilibria may be best analyzed by considering the overall reactions between the acid gas and the amine:

$$(I)\quad H_2S + RNH_2 = HS^- + RNH_3^+ \qquad (2.6)$$

$$(II)\quad RNH_2 + CO_2 + H_2O = RNH_3^+ + HCO_3^- \qquad (2.7)$$

The equilibrium constants for the overall reactions in the mixed and aqueous solvents are shown in Table 11.

Table 11

Equilibrium Constants for Overall Reactions in Mixed and Aqueous AMP

	40°C		100°C	
	mixed	aqueous	mixed	aqueous
K_I	84.9	439.	3.36	28.9
K_{II}	374.	1468.	5.35	37.4

A comparison of the equilibrium constants reflects the inhibiting effect of the physical solvent on the reaction between the acid gas and the amine.

The effect of the solvent on the chemical reactions may be further illustrated by examining the concentration of the species as a function of solution loading. The predicted molality of molecular H_2S, HS^-, S^{-2}, and undissociated AMP at 40 and 100°C is plotted versus solution loading in Figures 15 and 16. The total AMP molality in both solvents is 2.24 mol/kg. The undissociated H_2S and AMP are in higher concentration in the mixed solvent than in the aqueous solvent. At high loading the concentration of the undissociated H_2S in the mixed solvent approaches the concentration in the aqueous solvent.

The results of the correlation reaffirm the basic effects of the solvent on acid gas solubility. The difference in partial pressure of the acid gas above solutions of high loading is almost entirely due to the difference in the physical solubility (Henry's constants) between the mixed and aqueous systems. At loadings less than 1 mol/mol AMP, the increased physical solubility in the mixed solvent is offset by the decreased reaction of the acid gas in the liquid phase.

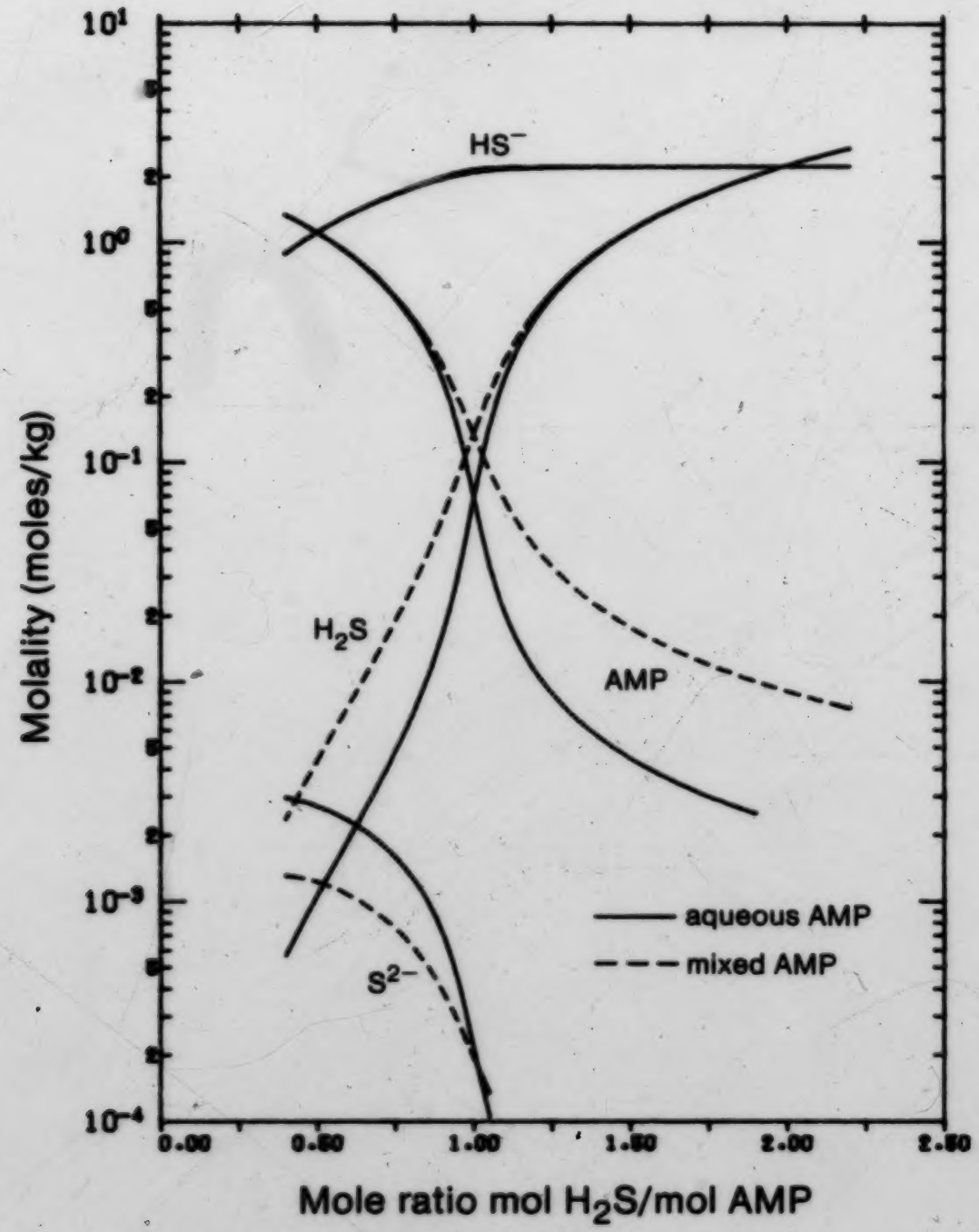

Figure 15 Concentration of liquid phase species at 40°C as a function of H_2S loading.

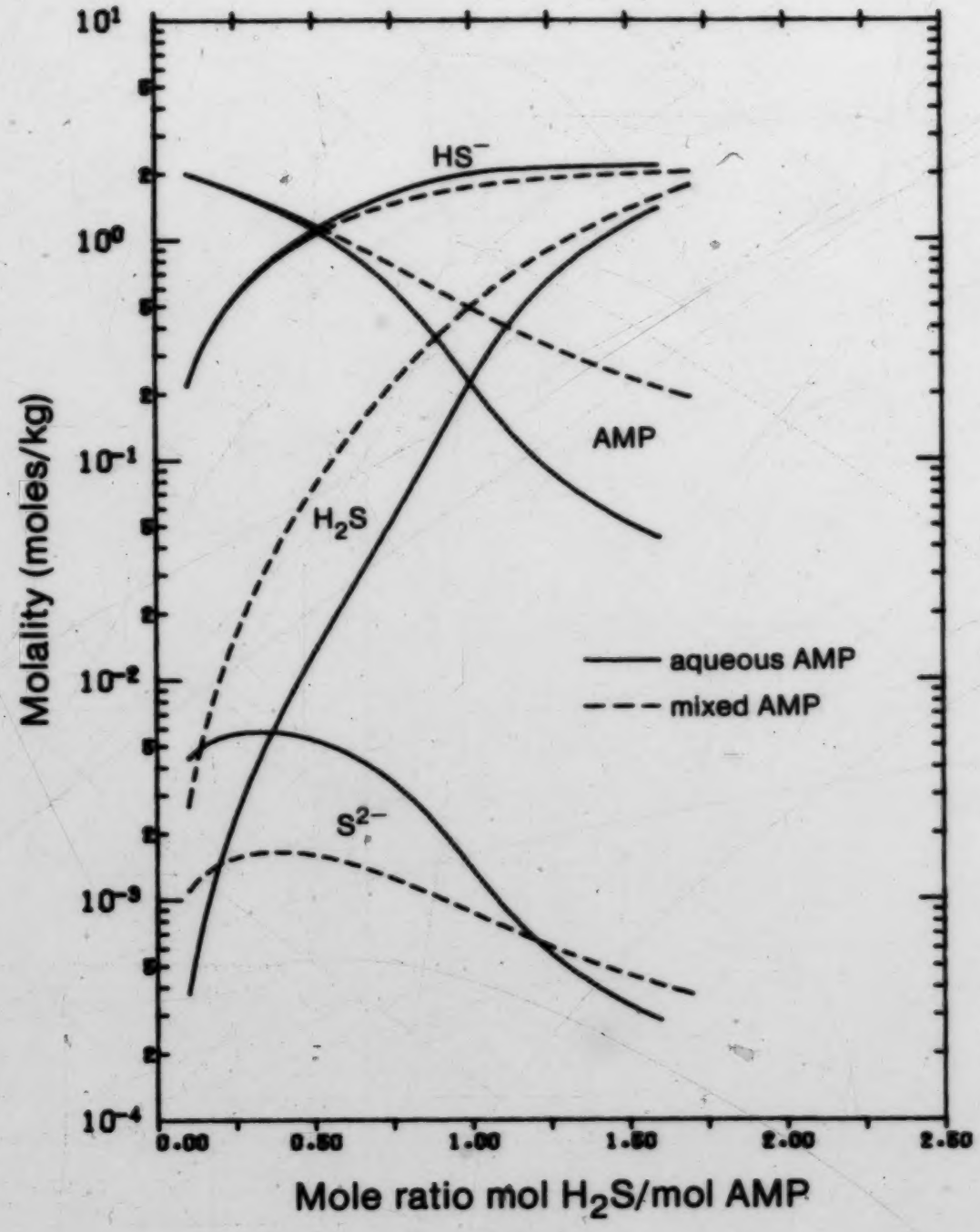

Figure 16 Concentration of liquid phase species at 100°C as a function of H_2S loading.

6. CONCLUSIONS

The equilibrium solubility of CO_2 and H_2S in a mixed solvent of AMP, sulfolane, and water, and in a solvent of AMP and water, has been measured at temperatures typical of the absorption and regeneration stages. The amine concentration in both solvents was 2.0 M thus permitting an evaluation of the influence of the physical solvent on the solubility behaviour.

The capacity for the acid gases is enhanced at high solution loading by the replacement of part of the water with sulfolane. The increase in solubility is more pronounced for H_2S than CO_2. At low solution loadings, the solubility of the acid gas in the mixed solvent is lower than in the corresponding aqueous system.

The solubility in the mixed solvent has been correlated by the application of a modified version of the method of Deshmukh and Mather. The modifications have accounted for the solvent effects on the physical vapour-liquid equilibria and on the chemical equilibria between reacting species. The predictions by the model are in excellent agreement with the experimental results.

The results of the solubility determination and the correlation are rationalized in terms of the solvent effects on the Henry's constant and on the chemical equilibrium constants. The replacement of a portion of the water with sulfolane increases the physical solubility of the acid gas. This replacement also reduces the dielectric constant of the

mixed solvent which inhibits the reaction between the acid gas and the amine. The two effects have opposite influences on the partial pressure of the acid gas above the solution. At high loadings, the influence of the chemical reaction is negligible, and the difference in solubility is due to the difference in the Henry's constants. At low loadings, the solvent effect on the chemical reaction is great enough to offset the increase in physical solubility and leads to a lower solubility in the mixed solvent.

References

1. Atwood, K., Arnold, M.R. and Kindrick, R.C., Ind. Eng. Chem., 49, 1439 (1957).

2. Banasiak, J., Gaz., Woda. Tech. Sanit., 55, 196 (1981).

3. Barbero, J.A., McCurdy, K.G. and Tremaine, P.R., Can. J. of Chem., 60, 1872 (1982).

4. Beutier, D. and Renon, H., Ind. Eng. Chem. Process. Des. Dev., 17, 220 (1978).

5. Bratzler, K. and Doerges, A., Hydrocarbon Processing, 53(4), 78 (1974).

6. Chen, C.C., Britt, H.I., Boston, J.F. and Evans, L.B., A. I. Ch. E. J., 25, 820 (1979).

7. Deshmukh, R.D. and Mather, A.E., Chem. Eng. Sci., 36, 355 (1981).

8. Dimov, V.E., Leites, I.L., Murzin, V.I., Yazvikova, N.V., Tyurina, L.S. and Sukhotina, A.S., Sov. Chem. Ind., 8, 211 (1976).

9. Dunn, C.L., Freitas, E.R., Goodenbour, J.W., Henderson, H.T., and Papadopoulous, M.N., Oil and Gas J., 62(11), 95 (1964).

10. Edwards, T.J., Newman, J. and Prausnitz, J.M., A. I. Ch. E. J., 21, 248 (1975).

11. Edwards, T.J., Maurer, G., Newman, J. and Prausnitz, J.M., A. I. Ch. E. J., 24, 966 (1978).

12. Hildebrand, J.H., Prausnitz, J.M., and Scott, R.L., "Regular and Related Solutions," Van Nostrand-Reinhold, New York, N.Y. (1970).

13. Isaacs, E.E., Otto, F.D. and Mather, A.E., J. Chem. Eng. Data, 22, 317 (1977).

14. Jones, J.H., Froning, H.R. and Claytor, Jr., E.E., J. Chem. Eng. Data, 4, 85 (1959).

15. Jou, F., Mather, A.E. and Otto, F.D., Ind. Eng. Chem. Process Des. Dev., 21, 539 (1982).

16. Lawson, J.D. and Garst, A.W., J. Chem. Eng. Data, 21, 20 (1976).

17. Lee, J.I., Otto, F.D. and Mather, A.E., J. Chem. Eng. Data, 17, 465 (1972).

18. Lee, J.I., Otto, F.D. and Mather, A.E., J. Chem. Eng. Data, 18, 71 (1973).

19. Lee, J.I. and Mather, A.E., Ber. Bunsenges. physik. Chem., 81, 1020 (1977).

20. Leites, I.L., Sichkova, O.P. and Shinelis, A.F., Khim. Prom., 48, 263 (1972).

21. Kent, R.L. and Eisenberg, B., Proc. Gas. Cond. Conf. 1975, 25, E1 (1975).

22. Klyamer, S.D., Kolesnikova, T.L. and Rodin, Yu.A., Gazov. Prom., 18, 44 (1973).

23. Kryukov, P.A., Starostina, L.I., Tarasenko, S.Ya. and Primanchuk, M.P., Geokhimiya, 7, 1003 (1974).

24. Mason, D.M. and Kao, R., in "Thermodynamics of Aqueous Systems with Industrial Applications," ed. by S.A. Newman, ACS Symposium Series 133 (1980).

25. Mason, J.W. and Dodge, B.F., Trans. A. I. Ch. E., 32, 27 (1936).

26. Nasir, P. and Mather, A.E., Can. J. Chem. Eng., 55, 715 (1977).

27. O'Connell, J.P. and Prausnitz, J.M., Ind. Eng. Chem. Fundam., 3, 347 (1964).

28. O'Connell, J.P., A. I. Ch. E. J., 17, 659, (1971).

29. Patterson, C.S., Slocum, G.H., Busey, R.H. and Mesmer, R.E., Geochimica et Cosmochimica Acta, 46, 1653 (1982).

30. Pitzer, K.S., J. Phys. Chem., 77, 268 (1973).

31. Prausnitz, J.M. and Shair, F.H., A. I. Ch. E. J., 7, 682 (1961).

32. Reed, R.M. and Wood, W.R., Trans. A. I. Ch. E., 37, 363 (1941).

33. Rivas, O., Ph. D. thesis, University of California, Berkeley, California (1978).

34. Ruska, W.E.A., Hurt, L.J. and Kobayashi, R., Rev. Sci. Instrum., 41, 1444 (1970).

35. Sartori, G. and Savage, D.W., Ind. Eng. Chem. Fundam., 22, 239 (1983).

36. Sen, B., Roy, R.N., Gibbons, J.J., Johnson, D.A., Adcock, L.H., "Thermodynamic Behaviour of Electrolytes in Mixed Solvents II," Adv. Chem. Ser. 177, 215 (1979).

37. Tiepel, E.W. and Gubbins, K.E., Can. J. Chem. Eng., 50, 361 (1972).

38. Tomcej, R.A., Otto, F.D. and Nolte, F.W., Proc. Gas Cond. Conf., Norman, Oklahoma 1983, 33, P1 (1983).

39. Van Krevelen, D.W., Hoftijzer, P.J. and Huntjens, F.Y., Rec. Trav. Chim., 68, 191 (1949).

40. Woertz, B.B., Can. J. Chem. Eng., 50, 425 (1972).

41. Woolley, E.M., Hurkot, D.G. and Hepler, L.G., J. Phys. Chem., 74, 3908 (1970).

42. Yushko, V.L., Sergienko, I.D., Kosyakov, N.E., Khokhlov, S.F., Pushkin, A.G., Ivanova, A.E. and Kosenko, E.D., Vop. Khim. Tekhnol., 30, 3 (1973).

Appendix 1. Gas Chromatograph Calibration

The gas chromatograph was calibrated by measuring the area percent response of mixtures of known composition. The mixtures of H_2S/N_2 and CO_2/N_2 were prepared by filling an evacuated tared sample cylinder with the gases. The cylinder was reweighed to the nearest 0.1 mg after the addition of each gas. The mass of each gas in the cylinder was determined and the mole percent of the acid gas calculated. The cylinder, which contained several stainless steel balls, was agitated and the gases allowed to mix for 4 to 5 hours. The cylinder contents were analyzed with the gas chromatograph conditions as outlined in Chapter 3. At least three analyses were performed for each gas mixture.

The response factors of the acid gases relative to N_2 were determined by Equation (A1.1).

$$RF = \frac{\text{area \% acid gas} \quad (100 - \text{mole \% acid gas})}{(100 - \text{area \% acid gas}) \quad \text{mole \% acid gas}} \qquad \text{(A1.1)}$$

The response factors varied with composition and increased with acid gas concentration. The results are shown in Tables A1.1 and A1.2.

Table A1.1

Variation of CO_2 Response Factors with Composition

Mixture	area %	mole %	RF
1.	11.68	10.53	1.123
2.	38.47	35,61	1.131
3.	54.61	51.09	1.152
4.	73.71	70.08	1.184
5.	93.28	92.31	1.184

Table A1.2

Variation of H_2S Response Factors with Composition

Mixture	area %	mole %	RF
1.	12.41	11.80	1.060
2.	22.14	21.09	1.064
3.	35.78	33.84	1.089
5.	70.32	67.89	1.120
6.	76.01	74.04	1.117
7.	84.41	81.80	1.204
8.	91.55	89.99	1.205

Appendix 2 - Calculation of Solubility from Measured Quantities

The calculations involved in the determination of the solubility of the acid gases in the solvents studied are outlined in the following sections. Typical values for the experimental quantities have been used.

1. H_2S content in liquid sample

Data:

volume of total sample: 100.0 cm^3
volume of aliquot sample: 10.00 cm^3
volume of 0.100 N iodine added: 20.00 cm^3
volume of 0.100 N thiosulphate required: 8.6 cm^3

moles H_2S in aliquot sample =

$$\frac{(20.00 - 8.6) \times 0.100}{2 \times 1000} = 5.70 \times 10^{-4} \text{ moles}$$

moles H_2S in total sample =

$$5.70 \times 10^{-4} \times \frac{100.0}{10.00} = 5.70 \times 10^{-3} \text{ moles}$$

2. CO_2 content in liquid sample

Data:

volume of total sample: 100.0 cm^3
volume of aliquot sample: 20.00 cm^3
mass of NaOH solution used: 29.4455 g
volume of 0.100 N HCl required: 15.3 cm^3
carbonate content of NaOH solution: 2.0×10^{-4} moles/g

moles CO_2 in aliquot sample=

$$\frac{15.3 \times 0.100}{2 \times 1000} = 7.65 \times 10^{-4} \text{ moles}$$

moles CO_2 in liquid sample and hydroxide solution =

$$7.65 \times 10^{-4} \times \frac{100.0}{20.00} = 3.83 \times 10^{-3} \text{ moles}$$

moles CO_2 in equilibrium liquid sample =

$3.82 \times 10^{-3} - (2.0 \times 10^{-4})(29.4455) = 3.77 \times 10^{-3}$ moles

3. Calculation of acid gas loading in aqueous and mixed amine solutions

Data

mass of sample: 3.3811 g
density of amine solution (23°C): .996 g/cm³
concentration of amine solution (23°C): 1.99 moles/l
moles CO_2 in sample: 3.77×10^{-3} moles

mass of lean amine solution =

$3.3811 - (3.77 \times 10^{-3})(44.0) = 3.2154$ g

moles amine =

$$\frac{3.2154 \times 1.99}{.996 \times 1000} = 6.42 \times 10^{-3} \text{ moles}$$

$$\alpha = \frac{3.77 \times 10^{-3}}{6.42 \times 10^{-3}} = 0.586 \text{ mol } CO_2/\text{mol AMP}$$

4. Calculation of acid gas content in sulfolane

Data:

mass of sample: 5.1195 g
moles CO_2 in sample: 1.43×10^{-3} moles

moles sulfolane in sample =

$$\frac{5.1195 - (1.43 \times 10^{-3})(44.0)}{120.17} = 4.21 \times 10^{-3} \text{ moles}$$

mole fraction CO_2 =

$$\frac{1.43 \times 10^{-3}}{1.43 \times 10^{-3} + 4.21 \times 10^{-2}} = 0.0329$$

5. Calculation of equilibrium partial pressure

Data:

cell pressure: 383.6 kPa
area % CO_2: 8.366 %
response factor: 1.123
water mole fraction (liq): 0.896
water sat. pressure: 7.38 kPa

mole fraction CO_2 =

$$\frac{8.366/1.123}{8.366/1.123 + (100 - 8.366)} = 0.0752$$

water partial pressure =

$0.896 \times 7.38 = 6.61$ kPa

partial pressure CO_2 =

$0.0752 \times (383.6 - 6.61) = 28.3$ kPa

Appendix 3 - Raw Experimental Data

Table A3.1 Raw Data - Solubility of Carbon Dioxide in 3.0 M Aqueous AMP at 40 C

Mass liquid sample (g)	Moles CO2 in liq.	AMP mol.	Moles AMP	x water	Mole ratio	Total P (kPa)	Partial P H2O (kPa)	y CO2	Partial P CO2 (kPa)
5.714E+00	6.62E-03	3.00	1.64E-02	0.905E+00	0.404E+00	4.80E+02	6.89E+00	0.264E-02	1.25E+00
3.544E+00	7.62E-03	3.00	9.69E-03	0.883E+00	0.786E+00	4.44E+02	6.52E+00	0.356E-01	1.56E+01
4.010E+00	1.03E-02	3.00	1.07E-02	0.873E+00	0.960E+00	4.48E+02	6.44E+00	0.817E+00	3.59E+02
4.599E+00	1.21E-02	3.00	1.23E-02	0.871E+00	0.982E+00	4.56E+02	6.43E+00	0.481E+00	2.18E+02
4.046E+00	1.03E-02	3.00	1.09E-02	0.873E+00	0.948E+00	4.61E+02	6.45E+00	0.317E+00	1.44E+02
4.513E+00	1.12E-02	3.00	1.21E-02	0.875E+00	0.919E+00	4.64E+02	6.48E+00	0.218E+00	9.95E+01
6.444E+00	1.46E-02	3.00	1.75E-02	0.880E+00	0.835E+00	3.91E+02	6.50E+00	0.953E-01	3.66E+01
2.376E+00	5.30E-03	3.00	6.47E-03	0.881E+00	0.818E+00	4.08E+02	6.50E+00	0.559E-01	2.25E+01
8.485E+00	1.70E-02	3.00	2.34E-02	0.886E+00	0.728E+00	4.00E+02	6.54E+00	0.327E-01	1.28E+01
5.039E+00	1.08E-02	3.00	1.38E-02	0.884E+00	0.769E+00	3.81E+02	6.52E+00	0.538E-01	1.90E+01
2.521E+00	4.26E-03	3.00	7.05E-03	0.893E+00	0.604E+00	3.55E+02	6.60E+00	0.102E-01	3.54E+00
7.088E+00	1.12E-02	3.00	1.99E-02	0.896E+00	0.564E+00	3.61E+02	6.61E+00	0.789E-02	2.79E+00

Table A3.2 Raw Data - Solubility of Carbon Dioxide in 2.0 M Mixed Solvent at 100 C

Mass liquid sample (g)	Moles CO2 in liq.	AMP mol.	Moles AMP	x water	Mole ratio	Total P (kPa)	Partial P H2O (kPa)	y CO2	Partial P CO2 (kPa)
2.826E+00	1.05E-03	1.98	5.14E-03	0.928E+00	0.204E+00	4.37E+02	9.40E+01	0.172E+00	5.89E+01
5.801E+00	3.07E-03	1.98	1.05E-02	0.923E+00	0.293E+00	4.80E+02	9.35E+01	0.291E+00	1.12E+02
6.775E+00	4.67E-03	1.98	1.21E-02	0.918E+00	0.384E+00	5.44E+02	9.30E+01	0.443E+00	2.00E+02
2.567E+00	2.34E-03	1.98	4.55E-03	0.911E+00	0.514E+00	6.79E+02	9.23E+01	0.610E+00	3.58E+02
4.365E+00	4.70E-03	1.98	7.69E-03	0.905E+00	0.611E+00	1.06E+03	9.18E+01	0.787E+00	7.60E+02
4.680E+00	6.72E-03	1.98	8.10E-03	0.894E+00	0.829E+00	1.83E+03	9.06E+01	0.892E+00	1.56E+03
7.908E+00	9.22E-04	1.98	1.45E-02	0.935E+00	0.634E-01	5.06E+02	9.48E+01	0.211E-01	8.70E+00
3.900E+00	9.49E-04	1.98	7.13E-03	0.932E+00	0.133E+00	4.88E+02	9.44E+01	0.751E-01	2.95E+01
5.098E+00	8.59E-03	1.98	8.73E-03	0.886E+00	0.984E+00	2.61E+03	8.98E+01	0.891E+00	2.24E+03
4.838E+00	9.28E-03	1.98	8.19E-03	0.878E+00	0.113E+01	3.95E+03	8.90E+01	0.936E+00	3.62E+03
4.985E+00	1.06E-02	1.98	8.35E-03	0.872E+00	0.127E+01	6.19E+03	8.83E+01	0.992E+00	6.05E+03

Table A3.3 Raw Data - Solubility of Carbon Dioxide in 2.0 M Mixed Solvent at 40 C

Mass liquid sample (g)	Moles CO2 in liq.	AMP mol.	Moles AMP	x water	Mole ratio	Total P (kPa)	Partial P H2O (kPa)	y CO2	Partial P CO2 (kPa)
4.357E+00	4.72E-03	1.98	7.67E-03	0.905E+00	0.615E+00	3.91E+02	6.68E+00	0.237E-01	9.14E+00
4.903E+00	6.73E-03	1.98	8.52E-03	0.896E+00	0.790E+00	3.84E+02	6.62E+00	0.752E-01	2.84E+01
4.447E+00	7.04E-03	1.98	7.65E-03	0.889E+00	0.920E+00	4.17E+02	6.57E+00	0.195E+00	7.99E+01
8.201E+00	1.35E-02	1.98	1.41E-02	0.887E+00	0.961E+00	4.80E+02	6.55E+00	0.382E+00	1.75E+02
5.200E+00	9.26E-03	1.98	8.86E-03	0.883E+00	0.105E+01	6.81E+02	6.52E+00	0.585E+00	3.94E+02
6.426E+00	1.22E-02	1.98	1.09E-02	0.879E+00	0.112E+01	1.15E+03	6.49E+00	0.822E+00	9.42E+02
7.139E+00	5.07E-03	1.98	1.28E-02	0.917E+00	0.397E+00	3.65E+02	6.77E+00	0.733E-02	2.63E+00
4.982E+00	4.78E-03	1.98	8.82E-03	0.908E+00	0.542E+00	3.83E+02	6.71E+00	0.142E-01	5.34E+00
4.774E+00	9.09E-03	1.98	8.08E-03	0.879E+00	0.112E+01	1.48E+03	6.49E+00	0.783E+00	1.15E+03
4.879E+00	1.02E-02	1.98	8.19E-03	0.873E+00	0.125E+01	2.77E+03	6.44E+00	0.905E+00	2.50E+03
3.427E+00	7.93E-03	1.98	5.69E-03	0.866E+00	0.139E+01	4.28E+03	6.39E+00	0.946E+00	4.05E+03
2.001E+00	5.30E-03	1.98	3.27E-03	0.855E+00	0.162E+01	5.82E+03	6.31E+00	0.968E+00	5.63E+03
2.182E+00	4.43E-03	2.00	3.71E-03	0.874E+00	0.119E+01	2.18E+03	6.46E+00	0.966E+00	2.10E+03
4.323E+00	9.48E-03	2.00	7.29E-03	0.869E+00	0.130E+01	3.46E+03	6.42E+00	0.981E+00	3.39E+03
3.236E+00	7.78E-03	2.00	5.40E-03	0.862E+00	0.144E+01	5.81E+03	6.37E+00	0.990E+00	5.74E+03
5.121E+00	9.10E-03	1.98	8.73E-03	0.883E+00	0.104E+01	5.74E+02	6.52E+00	0.843E+00	4.78E+02
5.334E+00	9.88E-03	1.98	9.06E-03	0.881E+00	0.109E+01	1.01E+03	6.50E+00	0.921E+00	9.29E+02
6.539E+00	1.29E-02	1.98	1.10E-02	0.877E+00	0.117E+01	1.91E+03	6.47E+00	0.962E+00	1.83E+03
5.345E+00	1.14E-02	1.98	8.96E-03	0.872E+00	0.127E+01	2.73E+03	6.44E+00	0.976E+00	2.66E+03
5.773E+00	1.31E-02	1.98	9.60E-03	0.867E+00	0.137E+01	3.67E+03	6.40E+00	0.983E+00	3.60E+03
5.346E+00	1.30E-02	1.98	8.82E-03	0.862E+00	0.148E+01	4.79E+03	6.36E+00	0.988E+00	4.73E+03
2.073E+00	5.45E-03	1.98	3.39E-03	0.855E+00	0.161E+01	6.16E+03	6.32E+00	0.992E+00	6.11E+03

Table A3.4 Raw Data - Solubility of Carbon Dioxide in 2.0 M Aqueous AMP at 40 C

Mass liquid sample (g)	Moles CO2 in liq.	AMP mol.	Moles AMP	x water	Mole ratio	Total P (kPa)	Partial P H2O (kPa)	y CO2	Partial P CO2 (kPa)
6.335E+00	6.01E-03	2.00	1.22E-02	0.938E+00	0.493E+00	4.58E+02	6.93E+00	0.480E-02	2.17E+00
4.120E+00	5.76E-03	2.00	7.76E-03	0.929E+00	0.742E+00	3.44E+02	6.86E+00	0.315E-01	1.08E+01
7.403E+00	1.31E-02	2.00	1.37E-02	0.921E+00	0.952E+00	3.78E+02	6.80E+00	0.257E+00	9.54E+01
6.016E+00	1.12E-02	2.00	1.11E-02	0.919E+00	0.101E+01	5.24E+02	6.78E+00	0.515E+00	2.68E+02
1.048E+00	2.04E-03	2.00	1.92E-03	0.917E+00	0.106E+01	8.82E+02	6.77E+00	0.746E+00	6.53E+02
5.545E+00	1.06E-02	2.00	1.02E-02	0.918E+00	0.104E+01	8.65E+02	6.78E+00	0.745E+00	6.40E+02
4.991E+00	1.03E-02	2.00	9.11E-03	0.914E+00	0.113E+01	2.00E+03	6.75E+00	0.904E+00	1.80E+03
7.044E+00	1.68E-02	2.00	1.27E-02	0.907E+00	0.133E+01	5.88E+03	6.70E+00	0.976E+00	5.74E+03
6.012E+00	8.30E-03	2.00	1.13E-02	0.929E+00	0.732E+00	3.81E+02	6.86E+00	0.256E-01	9.58E+00
3.530E+00	6.01E-03	2.00	6.56E-03	0.922E+00	0.916E+00	3.81E+02	6.81E+00	0.119E+00	4.45E+01
4.306E+00	8.55E-03	2.00	7.89E-03	0.916E+00	0.108E+01	1.42E+03	6.76E+00	0.804E+00	1.14E+03
3.968E+00	8.58E-03	2.00	7.21E-03	0.912E+00	0.119E+01	2.92E+03	6.74E+00	0.918E+00	2.68E+03

Table A3.5 Raw Data - Solubility of Carbon Dioxide in 2.0 M Aqueous AMP at 100 C

7.283E+00	1.97E-03	2.00	1.44E-02	0.952E+00	0.137E+00	4.36E+02	9.65E+01	0.251E-01	8.53E+00
6.575E+00	2.51E-03	2.00	1.30E-02	0.950E+00	0.193E+00	4.16E+02	9.63E+01	0.507E-01	1.62E+01
6.122E+00	3.50E-03	2.00	1.20E-02	0.946E+00	0.292E+00	4.09E+02	9.59E+01	0.113E+00	3.53E+01
3.948E+00	3.17E-03	2.00	7.85E-03	0.941E+00	0.414E+00	4.22E+02	9.54E+01	0.224E+00	7.32E+01
3.381E+00	3.76E-03	2.00	6.46E-03	0.935E+00	0.583E+00	4.95E+02	9.48E+01	0.429E+00	1.72E+02
6.260E+00	9.13E-03	2.00	1.18E-02	0.928E+00	0.776E+00	7.84E+02	9.40E+01	0.695E+00	4.66E+02
7.780E+00	1.43E-02	2.00	1.44E-02	0.919E+00	0.998E+00	1.61E+03	9.32E+01	0.877E+00	1.33E+03
2.892E+00	4.46E-03	1.98	5.36E-03	0.926E+00	0.832E+00	6.53E+02	9.39E+01	0.986E+00	5.51E+02
6.788E+00	1.12E-02	1.98	1.25E-02	0.924E+00	0.896E+00	9.88E+02	9.36E+01	0.991E+00	8.86E+02
5.990E+00	1.13E-02	1.98	1.09E-02	0.919E+00	0.103E+01	2.07E+03	9.31E+01	0.996E+00	1.97E+03
4.663E+00	9.78E-03	1.98	8.42E-03	0.914E+00	0.116E+01	3.84E+03	9.26E+01	0.997E+00	3.53E+03
6.164E+00	1.41E-02	1.98	1.10E-02	0.910E+00	0.127E+01	5.98E+03	9.22E+01	0.997E+00	5.87E+03

Table A3.6 Raw Data - Solubility of Hydrogen Sulphide in 2.0 M Mixed Solvent at 40 C

Mass liquid sample (g)	Moles H2S in liq.	AMP mol.	Moles AMP	x water	Mole ratio	Total P (kPa)	Partial P H20 (kPa)	y H2S	Partial P H2S (kPa)
6.506E+00	7.07E-03	1.98	1.16E-02	0.905E+00	0.611E+00	4.09E+02	6.69E+00	0.175E-01	7.06E+00
3.716E+00	6.10E-03	1.98	6.48E-03	0.888E+00	0.941E+00	4.00E+02	6.58E+00	0.140E+00	5.51E+01
2.522E+00	4.60E-03	1.98	4.37E-03	0.883E+00	0.105E+01	4.49E+02	6.52E+00	0.407E+00	1.80E+02
6.512E+00	5.70E-03	1.98	1.17E-02	0.912E+00	0.488E+00	4.44E+02	6.73E+00	0.561E-02	2.45E+00
8.495E+00	9.95E-03	1.98	1.51E-02	0.903E+00	0.660E+00	4.14E+02	6.67E+00	0.174E-01	7.09E+00
3.766E+00	5.50E-03	1.98	6.62E-03	0.894E+00	0.831E+00	4.96E+02	6.60E+00	0.451E-01	2.21E+01
5.800E+00	9.10E-03	1.98	1.01E-02	0.890E+00	0.897E+00	4.81E+02	6.58E+00	0.744E-01	3.53E+01
4.227E+00	7.25E-03	1.98	7.36E-03	0.886E+00	0.985E+00	4.67E+02	6.54E+00	0.200E+00	9.20E+01
3.681E+00	1.29E-02	1.98	5.99E-03	0.830E+00	0.215E+01	1.62E+03	6.13E+00	0.999E+00	1.61E+03
1.961E+00	6.20E-03	1.98	3.23E-03	0.841E+00	0.192E+01	1.40E+03	6.21E+00	0.999E+00	1.39E+03
3.478E+00	9.85E-03	1.98	5.81E-03	0.851E+00	0.170E+01	1.13E+03	6.29E+00	0.995E+00	1.11E+03
3.589E+00	8.95E-03	1.98	6.07E-03	0.862E+00	0.147E+01	7.85E+02	6.36E+00	0.995E+00	7.75E+02
3.747E+00	8.47E-03	1.98	6.39E-03	0.869E+00	0.133E+01	5.74E+02	6.42E+00	0.996E+00	5.65E+02
3.173E+00	6.45E-03	1.98	5.46E-03	0.876E+00	0.118E+01	3.53E+02	6.47E+00	0.997E+00	3.46E+02

Table A3.7 Raw Data - Solubility of Hydrogen Sulphide in 2.0 M Mixed Solvent at 100 C

Mass liquid sample (g)	Moles H2S in liq.	AMP mol.	Moles AMP	x water	Mole ratio	Total P (kPa)	Partial P H20 (kPa)	y H2S	Partial P H2S (kPa)
3.632E+00	1.45E-03	1.99	6.66E-03	0.926E+00	0.218E+00	4.21E+02	9.39E+01	0.494E-01	1.62E+01
7.085E+00	4.60E-03	1.99	1.29E-02	0.919E+00	0.357E+00	4.22E+02	9.31E+01	0.137E+00	4.51E+01
5.965E+00	5.70E-03	1.99	1.07E-02	0.909E+00	0.532E+00	4.62E+02	9.21E+01	0.297E+00	1.10E+02
8.382E+00	1.03E-02	1.99	1.49E-02	0.901E+00	0.694E+00	5.54E+02	9.13E+01	0.495E+00	2.29E+02
5.350E+00	8.85E-03	1.98	9.35E-03	0.888E+00	0.946E+00	8.10E+02	9.00E+01	0.989E+00	5.15E+02
3.223E+00	8.10E-03	1.98	5.59E-03	0.880E+00	0.109E+01	9.05E+02	8.92E+01	0.992E+00	8.09E+02
3.927E+00	8.45E-03	1.98	6.74E-03	0.872E+00	0.125E+01	1.30E+03	8.84E+01	0.994E+00	1.20E+03
3.682E+00	8.65E-03	1.98	6.27E-03	0.866E+00	0.138E+01	1.60E+03	8.78E+01	0.995E+00	1.50E+03
2.584E+00	7.10E-03	1.98	4.34E-03	0.854E+00	0.164E+01	2.29E+03	8.65E+01	0.996E+00	2.20E+03
9.542E+00	1.72E-03	1.98	1.76E-02	0.933E+00	0.979E-01	3.91E+02	9.48E+01	0.153E-01	4.53E+00
5.382E+00	1.20E-03	1.98	9.89E-03	0.932E+00	0.121E+00	3.94E+02	9.45E+01	0.207E-01	6.21E+00

Table A3.8 Raw Data - Solubility of Hydrogen Sulphide in 2.0 M Aqueous AMP at 100 C

Mass liquid sample (g)	Moles H2S in liq.	AMP mol.	Moles AMP	x water	Mole ratio	Total P (kPa)	Partial P H20 (kPa)	y H2S	Partial P H2S (kPa)
6.804E+00	1.00E-02	1.96	1.27E-02	0.929E+00	0.786E+00	8.21E+02	9.41E+01	0.358E+00	1.87E+02
3.346E+00	6.05E-03	1.98	6.18E-03	0.921E+00	0.979E+00	8.42E+02	9.34E+01	0.823E+00	4.66E+02
3.750E+00	7.72E-03	1.96	6.86E-03	0.916E+00	0.113E+01	1.30E+03	9.28E+01	0.788E+00	9.47E+02
4.987E+00	1.15E-02	1.96	9.04E-03	0.911E+00	0.128E+01	1.90E+03	9.23E+01	0.873E+00	1.58E+03
4.672E+00	1.18E-02	1.96	8.40E-03	0.906E+00	0.140E+01	2.12E+03	9.18E+01	0.992E+00	2.01E+03
6.443E+00	8.80E-03	2.00	1.25E-02	0.937E+00	0.529E+00	5.00E+02	9.50E+01	0.128E+00	5.18E+01
4.660E+00	6.67E-03	2.00	8.90E-03	0.929E+00	0.750E+00	5.38E+02	9.41E+01	0.335E+00	1.49E+02
7.289E+00	2.94E-03	2.00	1.44E-02	0.950E+00	0.203E+00	4.31E+02	9.83E+01	0.185E-01	5.51E+00
6.410E+00	6.30E-03	2.00	1.24E-02	0.938E+00	0.506E+00	5.75E+02	9.51E+01	0.664E-01	3.19E+01
5.681E+00	2.87E-03	2.00	1.12E-02	0.948E+00	0.256E+00	3.76E+02	9.80E+01	0.338E-01	9.40E+00
8.139E+00	2.27E-03	2.00	1.62E-02	0.952E+00	0.140E+00	4.90E+02	9.65E+01	0.573E-02	2.26E+00
7.477E+00	5.85E-03	2.00	1.48E-02	0.942E+00	0.400E+00	4.44E+02	9.55E+01	0.884E-01	2.39E+01

Table A3.9 Raw Data - Solubility of Hydrogen Sulphide in 2.0 M Aqueous AMP at 40 C

Mass liquid sample (g)	Moles H2S in liq.	AMP mol.	Moles AMP	x water	Mole ratio	Total P (kPa)	Partial P H20 (kPa)	y H2S	Partial P H2S (kPa)
2.680E+00	4.85E-03	1.98	5.00E-03	0.921E+00	0.970E+00	4.51E+02	6.80E+00	0.155E+00	6.88E+01
3.517E+00	6.67E-03	1.98	6.54E-03	0.919E+00	0.102E+01	5.29E+02	6.79E+00	0.340E+00	1.78E+02
2.126E+00	4.60E-03	1.98	3.91E-03	0.913E+00	0.118E+01	8.36E+02	6.75E+00	0.898E+00	5.66E+02
2.625E+00	6.85E-03	1.98	4.75E-03	0.904E+00	0.144E+01	1.34E+03	6.67E+00	0.959E+00	1.28E+03
6.000E+00	8.25E-03	1.98	1.14E-02	0.930E+00	0.726E+00	3.65E+02	6.87E+00	0.152E-01	5.46E+00
3.060E+00	4.80E-03	1.98	5.76E-03	0.926E+00	0.834E+00	5.70E+02	6.84E+00	0.232E-01	1.31E+01
3.335E+00	5.65E-03	1.98	6.25E-03	0.923E+00	0.905E+00	4.14E+02	6.82E+00	0.744E-01	3.03E+01
4.544E+00	9.32E-03	1.98	8.40E-03	0.916E+00	0.111E+01	7.41E+02	6.76E+00	0.518E+00	3.80E+02
4.394E+00	5.27E-03	1.98	8.38E-03	0.934E+00	0.630E+00	3.81E+02	6.89E+00	0.783E-02	2.93E+00
6.167E+00	9.22E-03	1.98	1.16E-02	0.928E+00	0.793E+00	4.24E+02	6.85E+00	0.235E-01	9.79E+00
7.196E+00	1.08E-02	1.98	1.36E-02	0.928E+00	0.794E+00	4.84E+02	6.85E+00	0.185E-01	8.82E+00
7.101E+00	8.37E-03	1.98	1.35E-02	0.934E+00	0.618E+00	4.61E+02	6.90E+00	0.592E-02	2.69E+00
3.863E+00	1.18E-02	1.98	6.88E-03	0.894E+00	0.172E+01	2.18E+03	6.60E+00	0.994E+00	2.16E+03
6.190E+00	1.67E-02	1.98	1.12E-02	0.902E+00	0.149E+01	1.49E+03	6.66E+00	0.995E+00	1.47E+03
4.681E+00	1.07E-02	1.98	8.54E-03	0.911E+00	0.125E+01	8.06E+02	6.72E+00	0.997E+00	7.97E+02

Table A3.10 Raw Data - Solubility of Carbon Dioxide in Sulfolane at 40 C

Mass liquid sample (g)	Moles CO2 in liq.	Moles Sulfolane	Liq. mole fraction	Total P (kPa)	Vapour mole fraction	Partial P (kPa)
5.120E+00	1.43E-03	4.21E-02	3.30E-02	4.42E+02	0.854E+00	3.77E+02
7.366E-01	1.98E-03	5.40E-03	2.68E-01	3.58E+03	0.984E+00	3.52E+03
6.910E-01	3.29E-03	4.54E-03	4.20E-01	5.61E+03	0.995E+00	5.58E+03
1.265E+00	4.39E-03	8.92E-03	3.30E-01	4.16E+03	0.995E+00	4.14E+03
2.552E+00	5.37E-03	1.93E-02	2.18E-01	2.53E+03	0.999E+00	2.53E+03
1.701E+00	1.46E-03	1.36E-02	9.66E-02	1.08E+03	0.999E+00	1.08E+03
5.220E+00	1.15E-03	4.30E-02	2.61E-02	4.84E+02	0.574E+00	2.78E+02
7.810E+00	1.16E-03	6.46E-02	1.77E-02	4.77E+02	0.388E+00	1.85E+02
4.653E+00	3.78E-04	3.86E-02	9.71E-03	4.98E+02	0.212E+00	1.06E+02
1.552E+00	1.93E-03	1.22E-02	1.36E-01	1.62E+03	0.993E+00	1.61E+03
5.731E+00	4.73E-04	4.75E-02	9.85E-03	4.85E+02	0.213E+00	1.03E+02

Table A3.11 Raw Data - Solubility of Carbon Dioxide in Sulfolane at 100 C

Mass liquid sample (g)	Moles CO2 in liq.	Moles Sulfolane	Liq. mole fraction	Total P (kPa)	Vapour mole fraction	Partial P (kPa)
2.818E+00	7.12E-04	2.32E-02	2.98E-02	7.74E+02	0.944E+00	7.31E+02
3.870E+00	1.92E-03	3.15E-02	5.74E-02	1.53E+03	0.994E+00	1.52E+03
4.304E+00	3.29E-03	3.46E-02	8.67E-02	2.36E+03	0.998E+00	2.36E+03
4.424E+00	6.55E-03	3.44E-02	1.60E-01	4.71E+03	0.997E+00	4.69E+03
3.894E+00	7.30E-03	2.97E-02	1.97E-01	5.92E+03	0.997E+00	5.90E+03
5.471E+00	7.86E-04	4.52E-02	1.71E-02	4.45E+02	0.998E+00	4.44E+02
5.936E+00	5.17E-04	4.92E-02	1.04E-02	4.04E+02	0.617E+00	2.49E+02

Table A3.12 Raw Data - Solubility of Hydrogen Sulphide in Sulfolane at 40 C

Mass liquid sample (g)	Moles H2S in liq.	Moles Sulfolane	Liq. mole fraction	Total P (kPa)	Vapour mole fraction	Partial P (kPa)
2.230E+00	2.18E-03	1.79E-02	1.09E-01	3.67E+02	0.711E+00	2.61E+02
2.983E+00	5.75E-03	2.33E-02	1.98E-01	6.21E+02	0.837E+00	5.20E+02
1.821E+00	1.01E-02	1.23E-02	4.53E-01	1.29E+03	0.987E+00	1.24E+03
1.486E+00	8.10E-03	1.05E-02	3.68E-01	9.84E+02	0.997E+00	9.81E+02
2.024E+00	8.28E-03	1.51E-02	2.93E-01	7.81E+02	0.999E+00	7.81E+02
2.097E+00	1.88E-02	1.30E-02	5.49E-01	1.81E+03	0.992E+00	1.80E+03
9.707E-01	1.14E-02	4.84E-03	7.02E-01	2.12E+03	0.988E+00	2.09E+03
8.978E+00	2.32E-03	4.91E-02	4.51E-02	4.28E+02	0.287E+00	1.23E+02

Table A3.13 Raw Data - Solubility of Hydrogen Sulphide in Sulfolane at 100 C

Mass liquid sample (g)	Moles H2S in liq.	Moles Sulfolane	Liq. mole fraction	Total P (kPa)	Vapour mole fraction	Partial P (kPa)
2.506E+00	4.40E-03	1.98E-02	1.83E-01	1.29E+03	0.990E+00	1.27E+03
3.690E+00	5.10E-03	3.09E-02	1.42E-01	1.04E+03	0.993E+00	1.04E+03
7.459E+00	3.40E-03	6.11E-02	5.27E-02	3.50E+02	0.994E+00	3.48E+02
4.933E+00	3.98E-03	3.60E-02	9.74E-02	7.24E+02	0.994E+00	7.20E+02
3.582E+00	7.75E-03	2.76E-02	2.19E-01	1.59E+03	0.995E+00	1.58E+03
1.258E+00	4.15E-03	9.29E-03	3.08E-01	2.37E+03	0.995E+00	2.35E+03

Appendix 4 - Error Analysis

1. Determination of acid gas loading in amine solutions

The calculation of the solution loading outlined in Appendix 2 may be generalized by defining the following variables:

T	equilibrium temperature (K)
V	volume of reagent (cm^3)
C_t	concentration of reagent (mol/l)
D	dilution factor
B	CO_2 background correction (mol CO_2)
W_s	mass of liquid sample (g)
C_s	amine concentration (mol AMP/g solution)
Mw	molecular weight of acid gas
m_{ag}	moles of acid gas
m_s	moles of solvent
α	mole ratio (mol acid gas/mol amine)

The solubility of the acid gases are calculated from the measured quantities by the following equations:

$$m_{ag} = \frac{V \cdot C_t \cdot D}{2 \cdot 1000} - B \qquad (A4.1)$$

$$m_s = (W_s - m_{ag} \cdot Mw) \cdot C_s \qquad (A4.2)$$

$$\alpha = \frac{m_{ag}}{m_s} \qquad (A4.3)$$

The uncertainty in the loading may be estimated by the following equations:

$$\Delta\alpha \cong \left|\left(\frac{\partial\alpha}{\partial V}\right)\Delta V\right| + \left|\left(\frac{\partial\alpha}{\partial B}\right)\Delta B\right| + \left|\left(\frac{\partial\alpha}{\partial C_s}\right)\Delta C_s\right| + \left|\left(\frac{\partial\alpha}{\partial T}\right)\Delta T\right| \qquad (A4.4)$$

$$\frac{\partial\alpha}{\partial C_s} = \frac{m_{ag}\,(W_s - m_{ag}\cdot Mw + B\cdot Mw)}{m_s^2} \qquad (A4.5)$$

$$\frac{\partial\alpha}{\partial B} = \frac{-m_s - m_{ag}\cdot C_s\cdot Mw}{m_s^2} \qquad (A4.6)$$

$$\frac{\partial\alpha}{\partial V} = \frac{C_t\cdot D\cdot(m_s + m_{ag}\cdot C_s\cdot Mw)}{2\cdot 1000\cdot m_s^2} \qquad (A4.7)$$

The average variation of loading with temperature is estimated at 0.008 K^{-1}. The estimated uncertainties in the measured values are:

ΔT = 0.10 K

ΔV = 0.20 cm^3

ΔB = 4.0 X 10^{-4} mol CO_2 (B = 0 for H_2S loading)

ΔC = 2.0 X 10^{-3} mol/g

Typical values for the remaining quantities are specified:

m_s = 0.00776 mol AMP

m_{ag} = 0.00576 mol CO_2

C_t = 0.1 mol/l

D = 5.0

V = 23.3 cm^3

W_s = 4.1205 g

B = 1.1 X 10^{-4} mol CO_2

α = 0.742 mol CO_2/mol AMP

From equations (A4.4) to (A4.7): $\Delta\alpha$ = 0.021 (2.8%)

2. Determination of partial pressure

The following variables are defined:

P_t total cell pressure (kPa)

y_a mole fraction acid gas

P_w partial pressure of water (kPa)

P_a partial pressure of acid gas (kPa)

The partial pressure of the acid gas is given by the equation:

$$P_a = y_a \cdot (P_t - P_w) \tag{A4.8}$$

The uncertainty in the partial pressure is given by equations (A4.9) to (A4.12).

$$\Delta P_a \cong \left|\left(\frac{\partial P_a}{\partial P_t}\right)\Delta P_t\right| + \left|\left(\frac{\partial P_a}{\partial P_w}\right)\Delta P_w\right| + \left|\left(\frac{\partial P_a}{\partial y_a}\right)\Delta y_a\right| \tag{A4.9}$$

$$\frac{\partial P_a}{\partial P_t} = y_a \tag{A4.10}$$

$$\frac{\partial P_a}{\partial P_w} = -y_a \tag{A4.11}$$

$$\frac{\partial P_a}{\partial y_a} = P_t - P_w \tag{A4.12}$$

The estimated individual uncertainties are:

ΔP_t = 10 kPa (P = 1 000 to 6 000 kPa)
= 1 kPa (P = 350 to 1 000 kPa)

ΔP_w = 3 kPa (at T = 100°C)
= 1 kPa (at T = 40°C)
= 0 (sulfolane)

Δy_a = .002

The error in partial pressure at 100°C is calculated for several experimental points using the above uncertainties and equations (A4.9 to A4.12).

P_t (kPa)	P_w (kPa)	y_a	P_a (kPa)	ΔP_a (kPa)	% ΔP_a
6000.	92.	.990	5850.	24.7	.42
2000.	92.	.960	1830.	16.3	.82
800.	92.	.700	495.	4.2	.85
350.	92.	.100	25.8	.92	3.5
350.	92.	.020	5.16	.58	11.

Appendix 5

Thermodynamic Framework

Reactions:

1. $RNH_3^+ = RNH_2 + H^+$
2. $2RNH_2 + CO_2 = RNH_3^+ + RNHCOO^-$
3. $H_2S = HS^- + H^+$
4. $HS^- = S^{-2} + H^+$
5. $CO_2 + H_2O = HCO_3^- + H^+$
6. $HCO_3^- = CO_3^{-2} + H^+$
7. $H_2O = H^+ + OH^-$

Chemical equilibrium expressions

$$K_1 = \frac{a_{RNH_2} \cdot a_{H^+}}{a_{RNH_3^+}} \qquad (A5.1)$$

$$K_2 = \frac{a_{RNH_3^+} \cdot a_{RNHCOO^-}}{a_{RNH_2}^2 \cdot a_{CO_2}} \qquad (A5.2)$$

$$K_3 = \frac{a_{HS^-} \cdot a_{H^+}}{a_{H_2S}} \qquad (A5.3)$$

$$K_4 = \frac{a_{S^{-2}} \cdot a_{H^+}}{a_{HS^-}} \qquad (A5.4)$$

$$K_5 = \frac{a_{HCO_3^-} \cdot a_{H^+}}{a_{CO_2} \cdot a_{H_2O}} \qquad (A5.5)$$

$$K_6 = \frac{a_{CO_3^{-2}} \cdot a_{H^+}}{a_{HCO_3^-}} \qquad (A5.6)$$

$$K_7 = \frac{a_{H^+} \cdot a_{OH^-}}{a_{H_2O}} \qquad (A5.7)$$

Activities are given for any species i, except water, by:

$$a_i = m_i \gamma_i \qquad \text{(A 5.8)}$$
$$\lim \gamma_i = 1$$
$$\Sigma m_j \rightarrow 0$$

where j represents any solute component. For water, the activity is defined as:

$$a_w = \gamma_w x_w \qquad \text{(A 5.9)}$$
$$\lim \gamma_w = 1$$
$$x_w \rightarrow 1$$

Vapour - liquid equilibrium expressions:

$$\phi_i y_i P = \gamma_i H_i m_i e^{\int_{P_w^s}^{P} \frac{\bar{v}_i}{RT} dP} \qquad \text{(A 5.10)}$$

$$\phi_w y_w P = \gamma_w x_w P_w^s \phi_w^s e^{\int_{P_w^s}^{P} \frac{\bar{v}_w}{RT} dP} \qquad \text{(A 5.11)}$$

The Poynting correction term may be approximated by:

$$e^{\frac{\bar{v}^{\infty}}{RT}(P - P_w^s)}$$

At the conditions of interest the vapour-liquid equilibrium expression for water may be simplified to:

$$y_w P = x_w P_w^s$$

Conservation equations

$$m_{H^+} + m_{RNH_3^+} = m_{OH^-} + m_{HCO_3^-} + m_{HS^-} + m_{RNHCOO^-} + 2(m_{S^{-2}} + m_{CO_3^{-2}}) \qquad \text{(A 5.12)}$$

$$m_{\text{total amine}} = m_{RNH_3^+} + m_{RNHCOO^-} + m_{RNH_2} \qquad \text{(A 5.13)}$$

$$m_{\text{total } CO_2} = m_{HCO_3^-} + m_{CO_3^{-2}} + m_{CO_2} \qquad \text{(A 5.14)}$$

$$m_{\text{total } H_2S} = m_{HS^-} + m_{S^{-2}} + m_{H_2S} \qquad \text{(A 5.15)}$$

$$y_{H_2S} + y_{CO_2} + y_{H_2O} = 1 \qquad \text{(A 5.16)}$$

Appendix 6 - Solubility Model Predictions

Table A6.1

Predicted Partial Pressure (kPa) of CO_2 in Aqueous and Mixed AMP Solutions at 40 and 100°C

	40°C		100°C	
α CO_2	Aqueous AMP	Mixed AMP	Aqueous AMP	Mixed AMP
0.10			4.28	19.2
0.20			16.6	64.5
0.30		1.44	37.3	134.
0.40		2.88	68.1	230.
0.50	1.95	5.16	113.	361.
0.60	4.05	8.82	180.	539.
0.70	8.24	15.1	285.	790.
0.80	17.7	27.7	472.	1140.
0.90	46.7	62.9	861.	1655.
1.0	251.	262.	1760.	2370.
1.10	1140.	996.	3480.	3330.
1.20	2320.	1970.	5960.	4540.
1.30	3700.	3090.		5990.
1.40		4396.		

Table A6.2

Predicted Partial Pressure (kPa) of H_2S in Aqueous and Mixed AMP Solutions at 40 and 100°C

	40°C		100°C	
α H_2S	Aqueous AMP	Mixed AMP	Aqueous AMP	Mixed AMP
0.10			1.13	3.61
0.20			4.52	13.5
0.30			11.0	31.2
0.40		1.58	22.1	59.4
0.50		2.91	40.6	101.
0.60	2.72	5.17	71.6	162.
0.70	4.99	9.26	125.	248.
0.80	9.83	17.4	221.	362.
0.90	23.8	37.0	402.	509.
1.00	99.7	90.0	725.	690.
1.10	358.	196.	1220.	903.
1.20	687.	333.	1860.	1140.
1.30	1040.	483.	2614.	1410.
1.40	1420.	639.		1700.
1.50	1830.	802.		2007.
1.60	2270.			2330.
1.70	2750.	1140.		2680.
1.80	3280.			
1.90		1500.		
2.10		1890.		

Table A6.3

Predicted H_2S Partial Pressure (kPa) in
2.0 M Mixed AMP at 40°C
as a Function of H_2S and CO_2 Loading

α H_2S	α CO_2			
	0.0	0.1	0.3	0.5
0.50	2.91	4.34	10.6	52.9
0.60	5.18	7.90	24.4	144.
0.70	9.26	15.1	68.3	265.
0.80	17.4	32.6	167.	398.
0.85	24.9	51.4	230.	468.
0.90	36.9	82.8	297.	541.
0.95	57.2	129.	366.	615.
1.00	90.0	187.	438.	692.
1.05	137.	252.	512.	771.
1.10	196.	322.	588.	852.
1.15	262.	394.	665.	936.
1.20	333.	469.	745.	1021.
1.30	483.	624.	909.	1200.
1.40	640.	785.	1080.	1390.
1.50	802.	952.	1260.	1600.
1.70	1140.	1300.	1640.	2030.
1.90	1500.	1680.	2060.	2540.
2.10	1887.	2082	2530.	3190.

Table A6.4

Predicted Effect of Temperature on the Solubility of H_2S in 2.0 M Mixed AMP Solution

	Partial Pressure (kPa)		
α H_2S	50°C	70°C	90°C
0.10			2.12
0.20		2.55	8.07
0.30	1.63	6.07	18.9
0.40	3.27	12.0	36.4
0.50	5.98	21.6	63.7
0.60	10.5	37.1	105.7
0.70	18.6	62.6	165.
0.80	34.1	105.	252.
0.85	47.1	135.	307.
0.90	66.5	174.	371.
0.95	95.2	223.	443.
1.00	136.	282.	525.
1.05	189.	351.	614.
1.10	253.	429.	712.
1.15	325.	515.	817.
1.20	404.	608.	930.
1.30	571.	810.	1170.
1.40	748.	1030.	1430.
1.50	933.	1260.	1720.
1.60	1120.	1500.	2020.
1.70	1320.	1760.	2320.
1.80	1530.	2020.	
1.90	1740.	2300.	
2.00	1960.		
2.10	2190.		

Table A6.5

Molality of Liquid Phase Species in 2.236 molal Mixed AMP at 40°C as a Function of H_2S Loading

α H_2S (mol/mol AMP)	Molality (moles/kg)			
	H_2S	HS^-	S^{-2}	AMP
0.40	2.360E-03	8.910E-01	1.310E-03	1.343E+00
0.50	4.360E-03	1.112E+00	1.220E-03	1.121E+00
0.60	7.757E-03	1.333E+00	1.065E-03	9.010E-01
0.70	1.388E-02	1.550E+00	8.600E-04	6.838E-01
0.75	1.885E-02	1.657E+00	7.500E-04	5.711E-01
0.80	2.613E-02	1.762E+00	6.330E-04	4.727E-01
0.85	3.729E-02	1.863E+00	5.110E-04	3.722E-01
0.90	5.528E-02	1.957E+00	3.907E-04	2.785E-01
0.95	8.534E-02	2.039E+00	2.811E-04	1.969E-01
1.00	1.340E-01	2.102E+00	1.936E-04	1.338E-01
1.05	2.038E-01	2.144E+00	1.340E-04	9.185E-02
1.10	2.899E-01	2.170E+00	9.710E-05	6.624E-02
1.15	3.860E-01	2.185E+00	7.400E-05	5.054E-02
1.20	4.877E-01	2.195E+00	5.900E-05	4.040E-02
1.30	6.994E-01	2.207E+00	4.200E-05	2.850E-02
1.40	9.160E-01	2.214E+00	3.238E-05	2.190E-02
1.50	1.136E+00	2.218E+00	2.600E-05	1.774E-02
1.70	1.578E+00	2.223E+00	1.900E-05	1.283E-02
1.90	2.022E+00	2.226E+00	1.500E-05	1.004E-02
2.10	2.468E+00	2.228E+00	1.220E-05	8.241E-03
2.20	2.691E+00	2.228E+00	1.122E-05	7.564E-03

Table A6.6

Molality of Liquid Phase Species in
2.236 molal Aqueous AMP at 40°C
as a Function of H_2S Loading

α H_2S (mol/mol AMP)	Molality (moles/kg)			
	H_2S	HS^-	S^{-2}	AMP
0.40	5.677E-04	8.909E-01	2.958E-03	1.339E+00
0.50	1.059E-03	1.114E+00	2.691E-03	1.116E+00
0.60	1.910E-03	1.337E+00	2.311E-03	8.939E-01
0.70	3.487E-03	1.560E+00	1.841E-03	6.724E-01
0.75	4.813E-03	1.671E+00	1.579E-03	5.622E-01
0.80	6.839E-03	1.781E+00	1.301E-03	4.527E-01
0.85	1.020E-02	1.889E+00	1.012E-03	3.446E-01
0.90	1.651E-02	1.995E+00	7.160E-04	2.394E-01
0.95	3.080E-02	2.093E+00	4.329E-04	1.422E-01
1.00	6.888E-02	2.167E+00	2.116E-04	6.866E-02
1.05	1.456E-01	2.202E+00	1.043E-04	3.366E-02
1.10	2.440E-01	2.216E+00	6.321E-05	2.035E-02
1.15	3.497E-01	2.222E+00	4.441E-05	1.429E-02
1.20	4.580E-01	2.225E+00	3.403E-05	1.094E-02
1.30	6.780E-01	2.229E+00	2.308E-05	7.418E-03
1.40	9.000E-01	2.230E+00	1.743E-05	5.600E-03
1.50	1.123E+00	2.231E+00	1.399E-05	4.495E-03
1.70	1.568E+00	2.233E+00	1.003E-05	3.221E-03
1.90	2.015E+00	2.233E+00	7.814E-06	2.509E-03

Table A6.7

Molality of Liquid Phase Species in 2.236 molal Mixed AMP at 100°C as a Function of H_2S Loading

α H_2S (mol/mol AMP)	Molality (moles/kg)			
	H_2S	HS^-	S^{-2}	AMP
0.10	2.666E-03	2.198E-01	1.108E-03	2.014E+00
0.15	5.712E-03	3.284E-01	1.310E-03	1.905E+00
0.20	1.000E-02	4.357E-01	1.461E-03	1.797E+00
0.30	2.306E-02	6.461E-01	1.616E-03	1.587E+00
0.40	4.373E-02	8.490E-01	1.647E-03	1.384E+00
0.50	7.468E-02	1.042E+00	1.589E-03	1.191E+00
0.60	1.192E-01	1.221E+00	1.472E-03	1.012E+00
0.70	1.810E-01	1.383E+00	1.322E-03	8.504E-01
0.80	2.633E-01	1.524E+00	1.161E-03	7.093E-01
0.90	3.679E-01	1.644E+00	1.005E-03	5.905E-01
1.00	4.945E-01	1.741E+00	8.658E-04	4.936E-01
1.10	6.408E-01	1.818E+00	7.469E-04	4.165E-01
1.20	8.034E-01	1.879E+00	6.486E-04	3.556E-01
1.30	9.789E-01	1.927E+00	5.682E-04	3.076E-01
1.40	1.164E+00	1.966E+00	5.027E-04	2.694E-01
1.50	1.357E+00	1.996E+00	4.490E-04	2.388E-01
1.60	1.556E+00	2.021E+00	4.045E-04	2.138E-01
1.70	1.759E+00	2.042E+00	3.674E-04	1.932E-01

Table A6.8

Molality of Liquid Phase Species in
2.236 molal Aqueous AMP at 100°C
as a Function of H_2S Loading

α H_2S (mol/mol AMP)	Molality (moles/kg)			
	H_2S	HS^-	S^{-2}	AMP
0.10	3.749E-04	2.188E-01	4.408E-03	2.007E+00
0.15	8.277E-04	3.295E-01	5.058E-03	1.896E+00
0.20	1.488E-03	4.402E-01	5.470E-03	1.784E+00
0.30	3.603E-03	6.614E-01	5.815E-03	1.563E+00
0.40	7.216E-03	8.815E-01	5.716E-03	1.343E+00
0.50	1.320E-02	1.099E+00	5.302E-03	1.126E+00
0.60	2.314E-02	1.314E+00	4.656E-03	9.128E-01
0.70	4.016E-02	1.521E+00	3.845E-03	7.070E-01
0.80	7.060E-02	1.715E+00	2.948E-03	5.148E-01
0.90	1.269E-01	1.883E+00	2.075E-03	3.484E-01
1.00	2.258E-01	2.009E+00	1.373E-03	2.244E-01
1.10	3.722E-01	2.086E+00	9.180E-04	1.477E-01
1.20	5.520E-01	2.131E+00	6.528E-04	1.041E-01
1.30	7.500E-01	2.156E+00	4.955E-04	7.866E-02
1.40	9.574E-01	2.173E+00	3.957E-04	6.262E-02
1.50	1.170E+00	2.184E+00	3.280E-04	5.180E-02
1.60	1.386E+00	2.191E+00	2.795E-04	4.407E-02

Table A6.9

Molality of Liquid Phase Species in
2.236 molal Mixed AMP at 40°C
as a Function of CO_2 Loading

α CO_2 (mol/mol AMP)	Molality (moles/kg)			
	CO_2	HCO_3^-	CO_3^{-2}	AMP
0.30	3.670E-04	4.234E-01	2.470E-01	1.318E+00
0.40	7.340E-04	6.324E-01	2.613E-01	1.081E+00
0.50	1.315E-03	8.613E-01	2.554E-01	8.638E-01
0.60	2.248E-03	1.107E+00	2.327E-01	6.639E-01
0.70	3.855E-03	1.366E+00	1.952E-01	4.794E-01
0.75	5.148E-03	1.500E+00	1.714E-01	3.927E-01
0.80	7.057E-03	1.636E+00	1.447E-01	3.103E-01
0.85	1.020E-02	1.776E+00	1.148E-01	2.308E-01
0.90	1.600E-02	1.914E+00	8.285E-02	1.567E-01
0.95	2.926E-02	2.044E+00	5.056E-02	9.050E-02
1.00	6.600E-02	2.146E+00	2.429E-02	4.171E-02
1.05	1.430E-01	2.193E+00	1.164E-02	1.960E-02
1.10	2.423E-01	2.210E+00	6.978E-03	1.167E-02
1.20	4.572E-01	2.222E+00	3.749E-03	6.242E-03
1.30	6.776E-01	2.227E+00	2.551E-03	4.240E-03
1.40	8.995E-01	2.229E+00	1.935E-03	3.210E-03

Table A6.10

Molality of Liquid Phase Species in 2.236 molal Aqueous AMP at 40°C as a Function of CO_2 Loading

α CO_2 (mol/mol AMP)	Molality (moles/kg)			
	CO_2	HCO_3^-	CO_3^{--}	AMP
0.50	4.262E-04	6.063E-01	5.112E-01	6.071E-01
0.60	8.807E-04	8.669E-01	4.738E-01	4.214E-01
0.70	1.786E-03	1.164E+00	3.990E-01	2.736E-01
0.75	2.578E-03	1.325E+00	3.494E-01	2.122E-01
0.80	3.807E-03	1.491E+00	2.932E-01	1.586E-01
0.85	5.927E-03	1.665E+00	2.301E-01	1.112E-01
0.90	1.005E-02	1.839E+00	1.629E-01	7.076E-02
0.95	2.030E-02	2.009E+00	9.475E-02	3.734E-02
1.00	5.436E-02	2.142E+00	3.978E-02	1.458E-02
1.05	1.346E-01	2.196E+00	1.684E-02	5.995E-03
1.10	2.368E-01	2.213E+00	9.727E-03	3.433E-03
1.20	4.541E-01	2.224E+00	5.135E-03	1.802E-03
1.30	6.755E-01	2.228E+00	3.476E-03	1.217E-03
1.40	8.979E-01	2.230E+00	2.620E-03	9.170E-04

Table A6.11

Molality of Liquid Phase Species in
2.236 molal Mixed AMP at 100°C
as a Function of CO_2 Loading

α CO_2 (mol/mol AMP)	Molality (moles/kg)			
	CO_2	HCO_3^-	CO_3^{-2}	AMP
0.05	9.505E-04	1.007E-01	1.016E-02	2.115E+00
0.10	3.195E-03	2.060E-01	1.438E-02	2.001E+00
0.15	6.482E-03	3.117E-01	1.726E-02	1.890E+00
0.20	1.074E-02	4.172E-01	1.927E-02	1.780E+00
0.30	2.223E-02	6.271E-01	2.147E-02	1.566E+00
0.40	3.813E-02	8.343E-01	2.192E-02	1.358E+00
0.50	5.961E-02	1.037E+00	2.111E-02	1.156E+00
0.60	8.871E-02	1.234E+00	1.937E-02	9.637E-01
0.70	1.288E-01	1.419E+00	1.700E-02	7.826E-01
0.80	1.850E-01	1.590E+00	1.428E-02	6.179E-01
0.90	2.640E-01	1.737E+00	1.154E-02	4.760E-01
1.00	3.710E-01	1.856E+00	9.097E-03	3.622E-01
1.10	5.083E-01	1.944E+00	7.146E-03	2.775E-01
1.20	6.704E-01	2.007E+00	5.698E-03	2.175E-01
1.30	8.510E-01	2.051E+00	4.651E-03	1.755E-01

Table A6.12

Molality of Liquid Phase Species in
2.236 molal Aqueous AMP at 100°C
as a Function of CO_2 Loading

α CO_2 (mol/mol AMP)	Molality (moles/kg)			
	CO_2	HCO_3^-	CO_3^{-2}	AMP
0.05	1.088E-04	6.417E-02	4.753E-02	2.075E+00
0.10	4.214E-04	1.504E-01	7.277E-02	1.939E+00
0.15	9.279E-04	2.448E-01	8.968E-02	1.811E+00
0.20	1.631E-03	3.443E-01	1.013E-01	1.689E+00
0.30	3.676E-03	5.536E-01	1.135E-01	1.455E+00
0.40	6.742E-03	7.722E-01	1.154E-01	1.233E+00
0.50	1.122E-02	9.969E-01	1.098E-01	1.019E+00
0.60	1.791E-02	1.225E+00	9.836E-02	8.138E-01
0.70	2.851E-02	1.455E+00	8.216E-02	6.171E-01
0.80	4.720E-02	1.679E+00	6.246E-02	4.319E-01
0.90	8.521E-02	1.886E+00	4.141E-02	2.674E-01
1.00	1.688E-01	2.044E+00	2.361E-02	1.452E-01
1.10	3.172E-01	2.129E+00	1.338E-02	8.023E-02
1.20	5.069E-01	2.168E+00	8.620E-03	5.112E-02